ELSEVIER

Cell Biology International 28 (2004) 913–933

Cell Biology International

www.elsevier.com/locate/cellbi

# Review and proposed action of alpha-fetoprotein growth inhibitory peptides as estrogen and cytoskeleton-associated factors

Gerald Mizejewski[a,*], George Smith[b], George Butterstein[b]

[a]*Division of Molecular Medicine, Wadsworth Center, New York State Department of Health, P.O. Box 509, Albany, 12201 NY, USA*
[b]*Department of Biological Sciences, Union College, Schenectady, NY, USA*

Received 10 May 2004; revised 7 July 2004; accepted 20 September 2004

**Abstract**

The (H) human growth-promoting factor, alpha-fetoprotein (AFP), has been reported to possess a growth inhibitory motif as an occult epitope in the compactly folded circulating form of the protein. Intermediate unfolded forms of the human HAFP molecule induced by stress, shock, and high ligand concentrations have revealed the presence of an encrypted growth-suppressive segment on the third domain of HAFP. A purified linear synthetic 34-mer segment termed the "growth inhibitory peptide" (GIP) exhibits various oligomeric forms with complex aggregation behaviors, in which dominant trimeric forms were found to be suppressive in assays of estrogen-induced growth. While several amino acid analogs of the cysteines of the GIP retained inhibitory activity, heavy metal binding and pre-incubation of the peptides with a variety of cations and hormone ligands were found to influence the outcomes of growth bioassays. Smaller segments of the original 34-mer were each found to display growth activities of their own, with the middle segment (P149b) also showing hydrophobic dye-binding properties. Studies of amino acid sequence identity further revealed that the GIP sequences displayed identity/similarity matches to both cytoplasmic and nucleus-cytoskeleton-associated proteins, and experimental evidence served to support these findings. That is, the peptide was capable of modulating tubulin polymerization, cell shape, and cell-surface aggregation phenomena reminiscent of a microtubule-associated protein. Immunofluorescence studies further pinpointed the localization of the GIP to cytoplasmic regions of high cytoskeletal density in the cell. Because of the involvement of the GIP in experimental models of the estrogen receptor/cytoskeleton, a mechanism of action is forwarded in which the linear GIP is proposed to be a G-coupled receptor binding ligand that is translocated across the plasma membrane via receptor-mediated endocytosis. Thus, it was predicted that the linear GIP and possibly its peptidic segments serve as decoy ligands to cell-surface receptors in order to gain access to the cytoplasmic compartment of the cell.


*Keywords:* Alpha-fetoprotein; Receptors; Peptides; Estrogen; Antigrowth; Uterus

## 1. Introduction

Human alpha-fetoprotein (HAFP) has been used in the clinical laboratory as a tumor and gestational-age-dependent fetal defect marker and is presently utilized as a screening agent for neural tube defects and aneuploidies (Abelev, 1971; Brock and Sutcliffe, 1972). In recent years, AFP has been determined to be a growth factor in both fetal and tumor environments (Li et al., 2002; Mizejewski, 2003). HAFP is a 70-kDa single-polypeptide chain containing 3–5% carbohydrate; it exhibits a triplicate domain structure configured by intramolecular loops dictated by disulfide bridging, resulting in a helical V- or U-shaped structure (Luft

* Corresponding author. Tel.: +1 518 486 5900.
*E-mail address:* mizejewski@wadsworth.org (G. Mizejewski).

1065-6995/$ - see front matter © 2004 International Federation for Cell Biology. Published by Elsevier Ltd. All rights reserved.
doi:10.1016/j.cellbi.2004.09.005

and Lorscheider, 1983; and cited in Mizejewski, 1997a, 2001a,b). The third domain of HAFP is known to contain a 34-amino acid (AA) segment that lies encrypted in the protein's native, compactly folded form (Mizejewski et al., 1996); this site is thought to become accessible via a conformational change involving a proposed rotational hinge (Morinaga et al., 1983). This hidden site has been shown to be decrypted by partial unfolding of the native full-length protein following exposure of the fetus to stress/shock environments (Butterstein et al., 2003b). The 34-amino acid sequence of the occult site has been identified and its synthetic peptide form has been purified, characterized, and assayed for biological activity (Mizejewski and MacColl, 2003). One major property of the 34-mer peptide was found to be suppression of growth in both neonatal and tumor cells; hence the name, growth inhibitory peptide (GIP). The growth-suppressive motif of the GIP on the HAFP has been demonstrated to function across vertebrate class boundaries: it is effective in the inhibition of thyroid-induced frog metamorphosis; it induces growth retardation in the fetal chick; and it suppresses estrogen-induced perinatal toxicity in rodents (Butterstein and Mizejewski, 1999; Butterstein et al., 2003b).

The human GIP has been reported to exhibit AA sequence identity/similarity to a number of stress and shock-related proteins. Such proteins are associated with anoxic, pH, ionic, hypertonic, and heat types of shock in addition to insulin/estrogen teratogenicity (Butterstein et al., 2003b). Although only ligand-binding effects (i.e. estrogens) of GIP epitope exposure on the HAFP molecules have been reported to date, it has been proposed that the other stress/shock conditions induce conformational changes in the native AFP protein (Bennett et al., 1993). In this regard, it has been demonstrated that both excess fatty acids and estradiol (E2) can induce a conformational change in native AFP that exposes the P149 epitope; this change is dependent upon the AFP/ligand molar ratios (Vallette et al., 1989; Haourigui et al., 1992). Since a subsegment of the GIP peptide (P149b) has previously been shown to bind E2 (Vakharia and Mizejewski, 2000), it is conceivable that E2 can diffuse into the molecular crevices of full-length, compactly folded HAFP as an initial binding interaction that initiates exposure of the P149b portion of the 34-mer GIP. Thus, the GIP site on the HAFP might represent a "hot-spot" that is sensitive to stress/shock conditions (e.g., excessive ligand concentrations) in the extracellular fluids and blood vascular compartments of the developing fetus. In protein–protein interactions, a molecular hot-spot has been defined as a small hydrophobic region (e.g. P149b) that dominates the free binding energy of a protein segment and is flanked by hydrophilic residues, in this case, P149a, and P149c to either side (see Fig. 1 and Table 1). In cells, however, stress/shock environments induce alterations in cellular form and shape; such alterations can be accomplished by activation of the intrinsic cytoskeletal proteins, i.e., actin, myosin, tubulin, and related microtubule proteins. Thus, stress/shock conditions can alter both the AFP molecule and the cellular environments in which the fetal protein is found.

In the present review, several models of in vivo and in vitro growth will be considered to further elucidate the estrogen-related biological roles of purified AFP-derived synthetic peptides, i.e., the GIP and its subsegments. Secondly, data from physio-chemical assays will be reviewed to demonstrate that the GIP and its hydrophobic subfragment (P149b) can bind and/or interact with both organic and biochemical agents. Thirdly, data will be surveyed to show that the GIP can influence estradiol (E2)-related cell cytoskeletal changes and hence, intracellular transport and cell shape. Fourthly, a genebank search is presented that revealed estrogen receptor, co-activators, and microtubular proteins showing amino acid sequence identity to GIP. Finally, the effects of GIP on endocrine- and cytoskeletal-sensitive growth which spans across vertebrate class boundaries will be reviewed in the hope of elucidating shared ligand-sensitive molecular targets and comparative mechanisms of action of the AFP-derived peptides.

## 2. GIP synthesis and characterization

The GIP and all other peptides were synthesized by F-MOC chemistry using an Applied Biosystems 431 A peptide synthesizer (Foster City, CA) as previously described (Mizejewski et al., 1996). In brief, the peptides were purified from the crude synthesis product by reverse-phase high-performance liquid chromatography (HPLC) (C-18 Delta PACK, 19 × 300 cm). A single peak (batch #P149) was obtained that was lyophilized and stored at 4 °C. The biochemical studies of the 34-mer P149 (GIP) established that the reverse-phase HPLC isolate was a reduced form of the peptide with a molecular mass of 3573 Da determined by electrospray ionization mass spectroscopy (Mizejewski et al., 1996). Subjection of the peptide to sequence analysis validated the AA positions. Circular dichroism (CD) in the far-UV range of the P149 peptide resulted in determination of secondary fine structure comprising 45% β-sheets and turns, 45% random coil, and 10% α-helix; moreover, computer modeling of GIP (Fig. 1B) supported the CD secondary fine structure (Wisconsin GCG software). Prior to use, aqueous solutions of peptide (0.1–1.0 mg/ml) were prepared fresh daily from lyophilized powder unless otherwise noted. Control peptides included a GIP-homologous peptide derived from the human albumin molecule (P263), and a scrambled version of the P149 peptide termed P237. Smaller peptide fragments of the 34-mer P149 were also synthesized and characterized

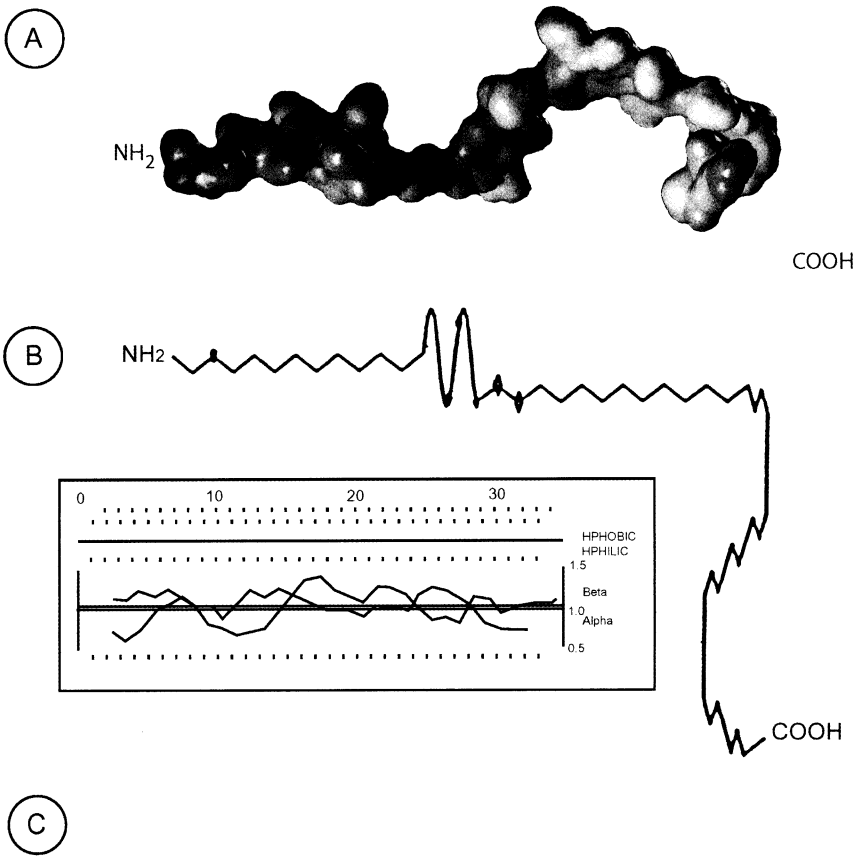


P149 (447-480) $NH_2$LSEDKLLACGEGAADIIIGHLCIRHEMTPVNPGVCOOH

P228 (447-458) $NH_2$LSEDKLLACGEGCOOH

P232 (459-472) $NH_2$AADIIIGHLCIRHECOOH

P211 (472-479) $NH_2$EMTPVNPGVCOOH

P237 (1-34) (scrambled) $NH_2$GINHLPSDAVGTAIEVMPCLRDGKLCIGAEHIELCOOH

Fig. 1. A composite diagram showing a minimal energy-derived computer model of the growth inhibitory peptide (GIP) (Panel-A); the diagram in Panel-B represents a secondary structure line model derived from the GCG Wisconsin Program together with an inset showing the hydrophilicity–hydrophobicity plot of the 34 amino acids of GIP (P149); note that the GIP is composed of a hydrophobic mid-piece with hydrophilic ends. (Panel-C) the amino acid sequence and composition of (P149); P228 (P149a); P232 (P149b); P211 (P149c), and P237, a scrambled version of P149. The minimal energy computer non-solvent model was kindly supplied by Dr. Curt Brennemen, Department of Chemistry, Rensselaer Polytechnic Institute, Troy, NY.

which included an amino terminal segment (P149a, 12 aa), a middle segment (P149b, 15 aa), and a carboxy terminal segment (P149c, 8 aa) (Fig. 1).

## 3. Comparison of peptide sequences

The AA sequences of the GIP-peptides, P149, P149a, P149b and P149c were compared with protein sequences derived from the genebank Swiss protein and PIR databases (Table 1) using the GCG (Wisconsin Program) FASTA sequence comparison software (Dauphinee and Mizejewski, 2002). Matches were found with proteins associated with the human estrogen receptor (HER), steroid receptor co-activators (SRC), cytoskeletal proteins, nuclear membrane proteins, annexins, and microtubule-associated proteins (Table 1). It should be noted that matches occurred with cytoskeletal

Table 1
Amino acid sequence matching of growth inhibitory peptide (P149) with various alpha-estrogen receptor, cytoplasmic and nuclear cytoskeletal-associated proteins

| I. Estrogen Receptor - Associated Proteins | | Percent (%) Identity/ Similarity | Percent (%) Total |
|---|---|---|---|
| HAFP 445 | L S E D K L L A C G E G A A D I I I G H L C I R H E M T P V N P G V G Q | 100/0 | 100 |
| Fragment P149 | ←——P149a——→←——P149b——→←→P149c——→ | | |
| Hum ER | X S M D K L L - C V E G M V E I - - - F V C L K - L N S G V | 54/21[a] | 75 |
| #395 | #401 #415 #445 #454 | | |
| Mus steroid coactivator | H R L L Q E G S Q P T P A Q P G V Y N | 42/32 | 74 |
| | #310 #925 | | |
| SRC-1 coactivator[a] | L T E D H I L | 58/42 | 100 |
| (I-III) #632-1434 | E S Q Q K L L | 42/42 | 84 |
| SRC-2 coactivator | L S E Q T L L | 71/14 | 85 |
| (I-III) #635-745 | D K K N K L L | 43/14 | 57 |
| SRC-3 coactivator | L S N N K L L | 58/42 | 100 |
| (I-III) #615-725 | E Q G H K L L | 43/14 | 57 |
| Mus caveolin #118 | I W I V V P C | 33/25 | 58 |
| HUM ER #505 | A Q L L L I L S H I R H X M S | 36/36 | 72 |
| II. Cytoplasmic Cytoskeleton - Associated Proteins | | | |
| Rat Nestin #1730 | G S E E S E S A S L E G E E G Q V T D H L D A P Q E V T S M V P G V G D | 38/18 | 54 |
| Hum Glycophorin #160 | L S E S K L L | 86/0 | 86 |
| Mus Moesin #46 | L A G D K L L | 71/14 | 85 |
| Hum Cofilin #82 | L S E C K P L | 71/0 | 71 |
| CL Annexin-1 | L S D E K L L A C | | |
| Hum -Actinin #957 | L S E Q R L L P R G E G | 75/16 | 91 |
| Mus Entactin #1935 | K L L S C G N H | 16/22 | 88 |
| Bovine Ezrin #60 | K L L S C G V W | 63/25 | 88 |
| Ferret Dynein #475 | E G Q A Q I I I G D L C V | 69/23 | 92 |
| Cut-7 Kinesin #810 | K A D I L H S H L | 63/25 | 88 |
| Hum RBC-P. Band 4.2 #110 | P A D A V I G H Y | 56/22 | 78 |
| P. Infest. Actin #475 | S L D I I V S H L | 56/33 | 89 |
| Hum Ankryin (Erythrocyte) | I D D I T V S H L | 44/22 | 66 |
| Hum Myosin-1 #1193 | I I I G Y L C T T | 66/11 | 77 |
| Yeast 5LA2P-Assemby #1300 | I I I S H L C R S | 66/11 | 77 |
| C.Elegan Kinesin #708 | C I F H E V T P F D | 60/20 | 80 |
| Hum Dystrophin #11729 | C I R K R L M P V A | 50/30 | 80 |
| C-Mechanosensory P10 #353 | | 31/46 | 77 |
| Hum Ankyrin #1306 | M M T P L K P G X G | | |
| Rat Gephyrin #338 | E M T P V L X G T E | | |
| Mus Kinesin #597 | G M T P L S P G T A | | |
| Hum Stratifin #162 | E M P P T N P I | 63/13 | 76 |
| Xenopus neurofil. Protein #675 | L M T P L N P L | 63/13 | 76 |
| D. Melano -tubulin #193 | P G I G N | 60/40 | 100 |
| III. Nuclear Cytoskeletal - Associated Proteins | | | |
| Hum Lamin- Receptor #470 | C P T W G G G A A S V D V G H D A V R H T P A V L L P G | 36/29 | 65 |
| Hum Nuclear Envelope-IMP #425 | G C G A A A A G R V R G R K C | 47/27 | 74 |
| Nuclear Hormone Receptor FtZ-F1 #628 | K P T P I S P G | 50/25 | 75 |

[a] SRC-1,-2, and -3 are consensus flanking sequences from the P160 coactivator family
Tubulin regulatory domain sequence: Similarity DKLLA - - - - - GHLCIR

Mus = mouse; Hum = human; ER = estrogen receptor; SRC = steroid receptor co-activator; CL = Columba livia; Cut = cutaneous RBC = red blood cell, P. infest = *Phytophthora infestans;* neurofil = neurofilament; D. melano = *Drosophilia melanogaster;* FTZ-F1 = nuclear transcription factor for AFP; # = number of the amino acid in the protein chain. The amino acid sequences of the alpha-fetoprotein growth inhibitory peptides (P149 and subsegments) were compared with the protein sequences derived from the genebank Swiss Protein and PIR databases using the GCG (Madison, Wisconsin) FASTA sequence comparison software. The FASTA program employs a Z-score statistic algorithm to demonstrate identity/similarity matches between two peptide amino acid sequences as previously described (Batrukova et al., 2000). For comparisons between short peptide sequences (<40 amino acids), a word score of 1–2 is employed with a default limit set at 2.0 and above. With the word score set, an *E* value of 1–10 is considered statistically significant. See references: Vakharia and Mizejewski (2000) and Butterstein et al. (2003a); for the SRC reference, see Torchia et al. (1997).

proteins such as ezrin, entactin, and actinin, as well as with motor proteins like kinesin, myosin, and dynein. Such motor proteins are known to participate in the transport of protein complexes and organelles throughout the cytoskeletal network. Also, a match can be seen with the HER in the region of its estrogen binding site (D-domain) and in segments of the steroid receptor co-activator (SRC) protein. Finally, matches exist with the nuclear envelope, the nuclear pore complex, and the inner nuclear membrane; all these proteins are involved in molecular size gating of the nuclear pores. Thus, the GIP segment contains sites that show identity/similarity to sequences in proteins related to ER function, motor proteins, and cytoskeletal and nuclear membrane proteins.

## 4. Estradiol-induced growth of the immature rodent uterus

An immature mouse uterine bioassay developed in the author's (GJM) laboratory was used to measure the growth inhibitory properties of HAFP and its derived peptides (Mizejewski et al., 1983, 1985). A rat uterine growth assay, employing 4.0 μg E2 administered to 16–18 day rat (45–50 g) pups, was adapted by Butterstein et al. (2003a) and used to study the antigrowth activity of the peptide bound to heavy metals. Peptide P149 was previously reported to suppress estradiol-induced growth in the immature mouse uterus (Table 2). The AFP-derived peptides inhibited (45–51%) E2-stimulated growth in the mouse

Table 2
Human alpha-fetoprotein (HAFP) and growth inhibitory peptides (GIP) tested in the 24 h immature mouse uterine growth bioassay with (W) and without (W/O) incubation in various treatment agents

| Peptide utilized | Number ($N$) of mice | Incubation and/or treatment agent | Percent (%) growth inhibition | Probability ($P$) value | Reference citation |
|---|---|---|---|---|---|
| 1. Native HAFP (cord | 15 | W estradiol (E2) | 32 | <.010 | Allen et al., 1993; |
| serum derived) | 15 | W/O estradiol | 0 | >.050 (NS) | Mizejewski and |
| | 8 | W estradiol; anti-HAFP antibody (Sera)[a] | 0 | >.050 (NS) | Jacobson, 1987; Bennett et al., 1993 |
| 2. Recombinant HAFP | 10 | W estradiol | 30 | <.025 | Bennett et al., 1997 |
| (*E. Coli* derived) | 10 | W/O estradiol | 0 | >.050 (NS) | |
| 3. P149 peptide (34-mer) | 20 | W estradiol | 51 | <.001 | Mizejewski, et al., 1996; |
| | 12 | W/O estradiol | 45 | <.010 | Vakharia and Mizejewski, |
| | 8 | Estradiol; anti-P149 antibody (Sera)[a] | 14 | >.050 (NS) | 2000; Mizejewski and MacColl, 2003 |
| 4. P149 peptide | 6 | W estradiol | 12 | >.050 (NS) | Unpublished data; |
| (cation addition) | | (a) $Ca^{++}$ ions | | | Butterstein et al., 2003a |
| | 6 | (b) $Mn^{++}$ ions | 16 | >.050 (NS) | |
| | 6 | (c) $Mg^{++}$ ions | 20 | >.050 (NS) | |
| 5. P149 peptide (derivatized) | | W estradiol | | | Eisele et al., 2001a,b |
| | 8 | Methylated ($CH_3$) cysteine | 31 | <.010 | |
| | 8 | Amindated ($NH_2$) cysteine | 29 | <.010 | |
| 6. P149 (plus ligands) | | W estradiol | | | Mizejewski, 1998 |
| | 5 | Retenoic acid | 23 | <.050 | Mizejewski, 1997a,b |
| | 5 | Vitamin-D | 33 | <.010 | Jacobson et al., 1999 |
| | 5 | T3-thyroid | 38 | <.010 | Bennett et al., 1993 |
| | 5 | Hydrocortisone | 31 | <.010 | |
| | 5 | Progesterone | 25 | <.025 | |
| 7. P149 peptide | 12 | W estradiol; W/O zinc | 39 | <.010 | Butterstein et al., 2003a |
| | 11 | W zinc | 43 | <.010 | |
| 8. P149 peptide cys mutations | | W estradiol | | | Eisele et al., 2001a,b |
| | 6 | Cys → ALA | 37 | <.050 | |
| | 6 | Cys → GLY | 17 | <.030 | |
| | 6 | Cys → SER | 0 | <.050 (NS) | |
| 9. P237 (scrambled GIP #1) | 10 | W/O estradiol | 0 | >.050 (NS) | Mizejewski et al., 1996 |
| P337 (scrambled GIP #2) | 9 | W estradiol | 0 | >.050 (NS) | Vakharia and Mizejewski, |
| | 9 | W/O estradiol | 0 | >.050 (NS) | 2000 |
| 10. P263 (albumin peptide) | 10 | W/O estradiol | 0 | >.050 (NS) | Mizejewski et al., 1996; |
| 11. P192 (C-terminus HAFP) | 10 | W/O estradiol | 0 | >.050 (NS) | Mizejewski and MacColl, |
| 12. P105 (non-related peptide) | 8 | W/O estradiol | 0 | >.050 (NS) | 2003 |

HAFP = Human alpha-fetoprotein; P149 = growth inhibitory peptide cation concentrations were 0.17 mg/l.
Cys → ALA = cysteine to alanine mutation.
[a] Intraperitoneal injection. All immature mice received at least one dose of E2; hormone ligands were incubated with GIP.

uterus from 100 ng to 1000 ng peptide per mouse; specifically, P149 and its fragments P149a and P149c significantly suppressed E2-induced uterine growth (Mizejewski et al., 1996; Vakharia and Mizejewski, 2000). In contrast, P149B only marginally suppressed uterine growth in the mouse (see Fig. 3). Similarly, the control peptides, a scrambled version of GIP (P237), and an albumin homologue of GIP (P263) did not inhibit uterine growth (<3%). Titration of a scrambled P237 peptide of the same amino acid composition failed to demonstrate activity at any dose studied (line #9). Likewise, a 40-mer peptide fashioned from the carboxy terminus of HAFP (P192, line #11) (residues 510–550) and a 34-mer peptide from a homologous region of human serum albumin (P263, line 10) showed no effect over this same range. These data show both the sensitivity and specificity of P149 as an inhibitor of E2-simulated growth in the immature mouse uterine growth assay.

Uterine growth assessment has also been utilized to determine the oligomeric state of GIP required for activity via the antigrowth assay. The purified 34-mer P149 exhibited complex aggregation behaviors; initially trimeric oligomers were formed that displayed growth inhibitory activity (Eisele et al., 2001a,b). The trimers, which can be separated by HPLC gel filtration (see Fig. 2, inset) slowly convert to dimers (disulfide bridge formation) that are inactive in the uterine antigrowth

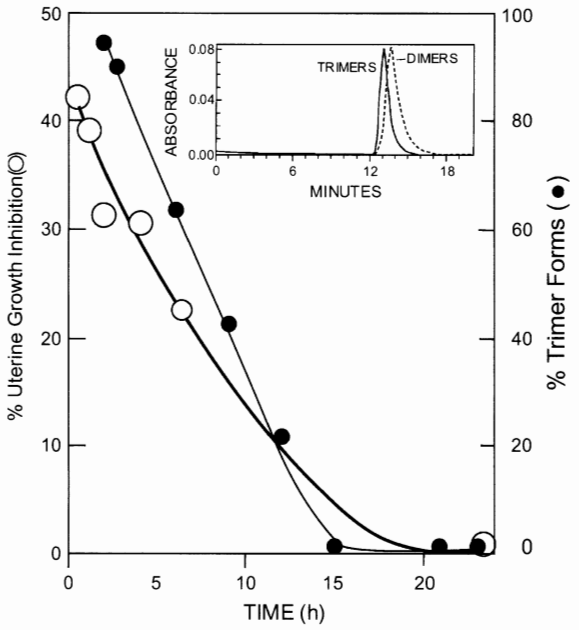


Fig. 2. The percent growth inhibition of P149 (left *y*-axis) in the immature mouse uterine assay is plotted in parallel with percent peptide trimer formation (right *y*-axis) as a function of time (*x*-axis). The inset demonstrates that the trimer can be distinguished from dimers by gel filtration HPLC methodology since the trimer-to-dimer conversion also occurs in a time dependent fashion. After 5 h, 50% of the inhibitory activity of P149 is lost, in parallel with a comparable loss of trimers. See references: Eisele et al., 2001a,b.

assay. The proportion of trimers was plotted against uterine growth inhibition at various time intervals of peptide solublized and stored in phosphate buffer. As shown in Fig. 2, the growth inhibitory potency of the GIP peptide decreased in parallel with the diminishing presence of trimer peptides in solution. Thus, the form of the linear peptide that was optimized for growth inhibition in the uterine bioassay was determined to be the trimer configuration (Eisele et al., 2001a). This was further confirmed by comparison of the individual oligomeric forms of GIP with inhibitory uterine growth potency together with peptide secondary structure using trifluoroethanol (TFE) exposure combined with amino acid mutation analysis (Table 3). Mutational amino acid/TFE analyses on the 34-mer peptides were previously described (Eisele et al., 2001a,b).

Prior studies have also provided evidence that the GIP (P149) derived from human AFP is intimately involved with down-regulation of E2-sensitive growth processes (Mizejewski et al., 1996; MacColl et al., 2001; Butterstein et al., 2003b). Although the antigrowth properties of the 34-mer GIP were originally described utilizing the immature rodent uterine bioassay, further properties of the GIP subsegments (P149a, P149b, P149c) have also been demonstrated (Vakharia and Mizejewski, 2000). Results clearly indicate that each peptidic segment of the P149 peptide possessed slightly differing inhibitory potencies; however, the sum of its parts did not equal the whole (Fig. 3). It was also observed (Table 2) that the presence of cationic ions ($Ca^{++}$, $Mg^{++}$, $Mn^{++}$) in the incubation media tended to reduce the inhibitory capability of GIP in the antigrowth assay. Further, it was shown that pre-incubation of the GIP with other hormones could also modify assay outcome as reported for HAFP (Bennett et al., 1993). Finally, it was apparent that the full-length, native, and recombinant AFP molecules required the presence of a high molar E2 excess for induction of the growth inhibitory property (Bennett et al., 1997), while purified GIP and its fragments did not require E2 incubation to produce its antigrowth activity (Mizejewski et al., 1996).

Table 3
The monomeric, oligomeric, and polymeric forms of the 34-mer growth inhibitory peptide (GIP) are charted versus their uterine growth inhibitory potency and their secondary structure determined by circular dichroism (CD)

| Form of peptide | C-peptide Percent growth inhibition (CD) | A-peptide Percent growth inhibition (CD) | G-peptide Percent growth inhibition (CD) | S-peptide Percent growth inhibition (CD) | HA-peptide Percent growth inhibition (CD) |
|---|---|---|---|---|---|
| A. Monomer | (11%, 33%) | (9%, 34%) | (10%, 34%) | (10%, 34%) | (9%, 35%) |
| 1. Methylated | 29.0 | Not done | Not done | Not done | Not done |
| 2. Amindated | 31.0 | | | | |
| B. Dimer[a] (inactive) | 6.0 (10%, 38%) | Not formed | 17.0 (27%, 19%) | 0.0 (10%, 34%) | 6.0 (Projected) |
| C. Trimer[a] (active) | 40.0 (32%, 18%)[c] | 37.0 (38%, 14%) | Not formed | Not formed | Not formed |
| D. Hexamer (active) | 37.0(32%, 18%)[c] | Not formed | Not formed | Not formed | Not formed |
| E. Trimer[a] plus hexamer[b] | 35.0 | Not done | Not formed | Not formed | Not formed |
| F. Trimer plus polymer[b] | <1.0 | Not done | Not formed | Not formed | Not formed |
| G. Polymer[a] | <1.0 | Not formed | Not formed | Not formed | Not formed |

Note that various amino acid mutations produce only certain oligomers. (10%, 38%) = percent (%) alpha-helix, (%) β-sheet, no trifluoroethanol; (32%, 18%) presence of 50% trifluoroethanol. Polymers = large aggregates (minimum size = 102 peptides (34-mer).

[a] Determined by high pressure gel-filtration column chromatography. C-peptides, cysteines are intact; A-peptide, cysteine to alanine mutation; G-peptide, cysteine to glycine mutation, S-peptide, cysteine to serine mutation. HA peptide = histidines mutated to alanines. (Projected) = the histidine to alanine mutation forms a dimer, a form which was previously inactive.

[b] Note that mixing trimer with polymer destroys growth inhibition property while mixtures of trimers and hexamers do not do so.

[c] Note: addition of trifluorethanol to the various peptide increases the α-helix while decreasing the β-sheet content. A similar reaction is known to occur when pore-forming peptides encounter the cell membrane lipid bilayer (Matsuzaki et al., 1989). See text: Section 10.

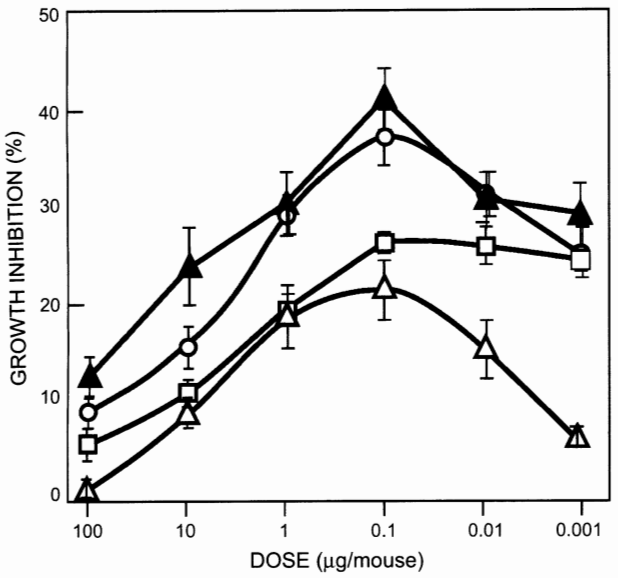


Fig. 3. A set of dose–response curves is depicted for alpha-fetoprotein derived Growth Inhibitory Peptide (P149) and its subsegments (P149a, P149b, P149c) in the immature mouse uterine growth assay. As shown in the graph, the peak growth inhibitory potency (38–42%) attained by P149 (○) and subsegment P149c (▲) at 0.1 to 1.0 μg administered per mouse for the 24-h assay. While subsegment P149a (□) achieved growth suppression of 25–28% at less than 0.1 μg/mouse, P149b (△) (the hydrophobic mid-piece) sustained only 18–22% inhibition at 0.1–1.0 μg/mouse. These data indicate that all three subsegments contribute, in some way, to the overall growth inhibitory potency of the 34-mer growth inhibitory peptide. Number ($N$) of animals at each point represent 6–10 determinations.

However, incubation of the GIP in E2 did slightly increase its growth inhibitory potency (Table 2).

Observations on the antiestrogenic growth effect displayed by GIP and its segments deserve further consideration. Since the first report of the antigrowth properties of the GIP was published (Mizejewski et al., 1996) a suitable explanation for this mode of activity has remained elusive. However, it was subsequently reported that both the 34-mer P149 and its P149a segment displayed a binding affinity ($10^{-6}$ M) for the HER, while P149b and P149c lacked this property (Vakharia and Mizejewski, 2000). Data also demonstrated that E2-induced in vivo growth inhibitory ability of both the P149 peptide and intact HAFP can be abolished by the use of a pre-injection bolus of anti-P149/anti-HAFP antibodies, respectively (Table 2). Abrogation of the antigrowth activity by antibody intervention suggests that the P149 antigrowth activity is neutralized either at the cell surface or in the blood circulation. In either event, complexing of P149 and/or HAFP with their respective antibodies prevented estrogen-sensitive growth inhibition by GIP/AFP in the immature mouse uterus. These data indicate that the antigrowth effect is initiated as a cell-surface event. Such a mode of action would require that quenching of the estrogenic growth stimulation of the cell involves an intracellular downstream uncoupling of a signal transduction cascade extending from the plasma membrane to the nucleus.

In view of the ER involvement, it has been established that isotypic forms of the human estrogen receptor-α (ERα) are located both in the nucleus and at the cell-surface membrane; these sites mediate estrogen-dependent genomic and nongenomic signaling, respectively (Acconcia et al., 2003; Watson et al., 2002); however, the membrane-associated ERα constitutes a smaller population of the total ER expressed in epithelial cells (Razandi et al., 2003a; Segars and Driggers, 2002). Moreover, the membrane (M) isoform can only activate the ER response element in the presence of estrogen, and MER entry into the nucleus was found to be gated by estrogen (Xu et al., 2004). It has been demonstrated that MER is also capable of nuclear genomic function and that its transcriptional activity occurs following hormone-dependent entry into the inner nuclear membrane where the receptor remains to initiate further nucleoplasmic interaction. Thus, the MER can interact with the transcriptional apparatus while positioned at the inner nuclear membrane and with membranous channels that form the heterochromatin-nuclear tubular network. The plasma membrane-tethered ERα is a nonintegral membrane protein associated with both caveolae and lipid rafts (see below) located at the cytoplasmic interface of the plasma membrane (Razandi et al., 2003b; Huo et al., 2003). The MER activation by estrogen binding can also affect nongenomic signal transduction events, such as the MAP kinase pathways (Baldi et al., 1986). Upon E2 binding to the cell-surface ER, the MER dissociates from its membrane-tethered complex and is transported as a caveolar vesicle complex through the cytoplasm via the cytoskeleton. The caveosome vesicle then merges and fuses with the smooth endoplasmic reticulum which is contiguous with the area of the nuclear pores, (perinuclear location), lodging onto the inner nuclear membrane (Pelkmans et al., 2001; Pyrpasopoulou et al., 1996). From the inner nuclear membrane, the MER has been shown to initiate the transcription process, and from here it acts in a manner similar to that of the canonical nuclear form of the HER (Xu et al., 2004) (see Fig. 7).

Caveolae are flask-shaped invaginations of the plasma membrane that constitute vesicular organelles. These integral membrane vesicles have a characteristic diameter of 50–100 nm and comprise 20% of the total plasma membrane surface area (Couett et al., 1997). Caveolae are present in most cell types and are implicated in cellular transcytosis, cholesterol trafficking, and signal transduction events. These invaginated vesicles are coated with the caveolin membrane protein and contain specific lipids (glycosphinolipids, sphingomyelin, and cholesterol) and lipid-modified signaling

molecules (Engelman et al., 1998). Caveolin proteins are mostly in plasma membranes but also occur in the Golgi, endosplasmic reticulum, in vesicles, and cytosolic locations (Williams and Lisanti, 2004). Caveolar membranes contain high levels of lipid rafts which have been characterized as cholesterol and glycosphingolipid-enriched micro-domains of the plasma membrane. The lipid rafts form liquid-ordered subdomains of decreased membrane fluidity. The long saturated lipid tails of the sphingolipids impart to the lipid rafts a high degree of order further stabilized by the interaction with cholesterol, bestowing a buoyancy to the bilayer (Huo et al., 2003). Interestingly, estrogen regulates both the number of caveolae and the levels of the caveolin protein in uterine smooth muscle (Turi et al., 2001). Thus, the formation and number of caveolae are influenced by the physiological state of the uterus in a steroid hormone-dependent manner.

Nuclear receptors (NR) require co-activator proteins to efficiently activate transcription of target genes (Onate et al., 1995; Heery et al., 1997). Binding of the estrogen to the ER is responsible for inducing a conformational change leading to transcription activation (TA) for that specific target gene (Gee et al., 1999; Geistlinger et al., 2004). The conformational change in the ligand-binding domain of the ER in response to hormone binding is responsible for recruitment of co-activator proteins that are required for TA by the E2 receptor (Bramlett and Burns, 2002). The ER co-activator P160 utilizes a short NR amino acid box motif to recognize the ligand-binding domain of the NR when activated by ligand (Bramlett et al., 2001). The P160 utilizes the conserved NR-box which has the core sequence LXXLL (L = leucine, X = any amino acid) flanked by less conserved sequences (Heery et al., 1997). Although the LXXLL motif is necessary to mediate the binding of these proteins to the E2-liganded nuclear receptors (NR), amino acid residues flanking the core motif are also important in the recognition of the various NRs (Savkur and Burris, 2004). It is of interest in the present context, that the P149a segment of the GIP shows sequence identity and similarity to the peptide stretches in P160 estrogen receptor co-activator (SRC-1,2,3) NR-box which constitute the aminoterminal flanking sequences of that motif (see Table 1).

## 5. Immunofluorescent localization

In order to localize the P149 in cells, immature uterine mouse tissues were subjected to immunohistochemistry using the double antibody immunofluorescence technique (Mizejewski and MacColl, 2003). Twenty-four hours following the immature uterine bioassay, the entire uteri from estrogen-, peptide-, and AFP-treated 15 day female mouse pups were frozen, and mounted for cryostat sectioning. Fluorescence localization of both P149 peptide and HAFP demonstrated similar fluorescent patterns. Localization of AFP and the P149 peptide can be observed in both stromal and epithelial cells of the immature mouse uterus (Fig. 4). A diffuse, glowing fluorescence was seen in the cytoplasm

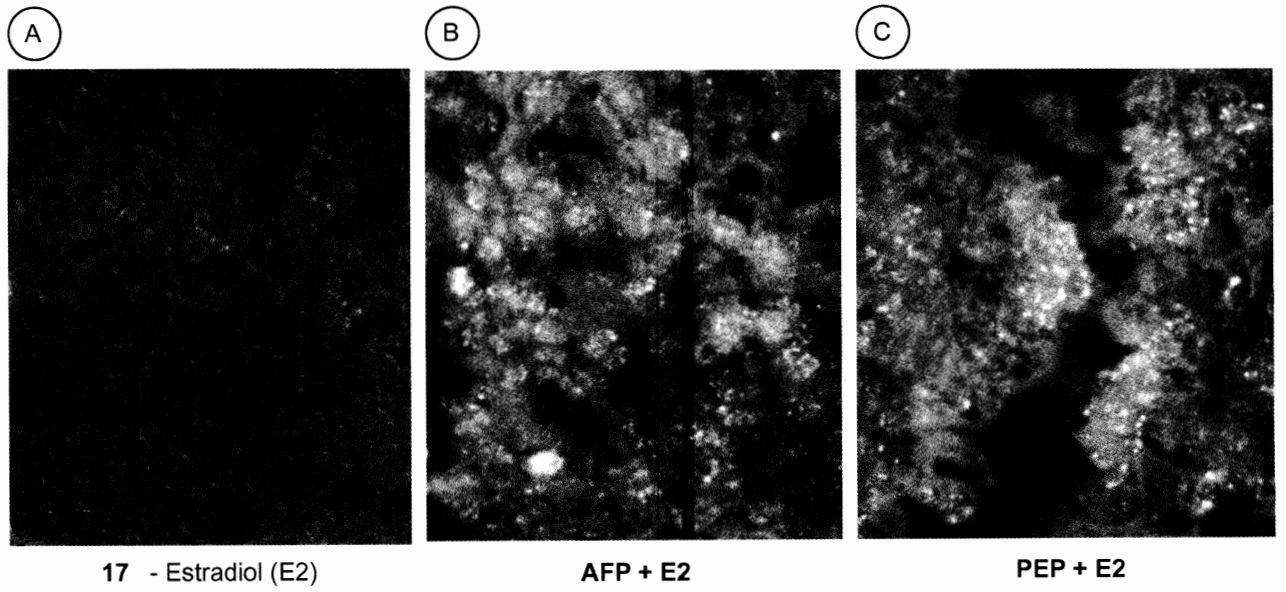


Fig. 4. Immature mouse uterine tissue and cells were biopsied 24 h following the injection of either estradiol (E2) alone (left panel), alpha-fetoprotein (AFP) plus E2, or peptide (P149) plus E2. Excised uteri were frozen and prepared by cryostat sectioning for double antibody immunofluorescent detection of AFP and P149, using their respective antibodies (see text). While E2 alone showed only background fluorescence, AFP and P149 both showed cytoplasmic and perinuclear fluorescent localization. The estrogen receptor is known to reside in both epithelial and stromal cells of the uterus (Cheng et al., 2004).

and fluorescence was also visible in the perinuclear region surrounding and outlining the nucleus (Fig. 4). In other studies, anti-tubulin antibodies were employed to visualize the cytoskeletal framework of the cell in both the cytoplasm and in the perinuclear regions (see below and Fig. 5).

Proteins, ligands, and viruses (SV40) have been reported to be internalized to the endoplasmic reticulum (EPR) by caveolae/raft-mediated endocytosis (Le and Nabi, 2003). Caveolin-1 is a recruiter of cargo to the endocytic caveolar domain. The caveolin-1 protein is ubiquitous, with the highest levels found in endothelia and smooth muscle cells (Williams and Lisanti, 2004). The endocytotic passage occurs in a microtubule-dependent fashion via caveolin-1 coated intermediate vesicles (Parton, 2003). After budding from the plasma membrane, passage of the caveosome and subsequent fusion with the smooth EPR require only 5 min and are associated with tyrosine kinase activation, actin filament assembly/disassembly, and dynamin recruitment. It is known that actin filaments play an accessory role in promoting the endocytotic process (Fujimoto et al., 2000). Following direct passage from the cell membrane and fusion with the EPR, expression of caveolin-positive vesicular structures has been identified in the perinuclear region of the cell (Pelkmans et al., 2001).

Since fluorescence was observed in the cytoplasm and in the perinuclear regions, it is evident that the peptide P149 achieved cytoplasmic residence (endocytosis). Since the peptide fluorescence was localized in both

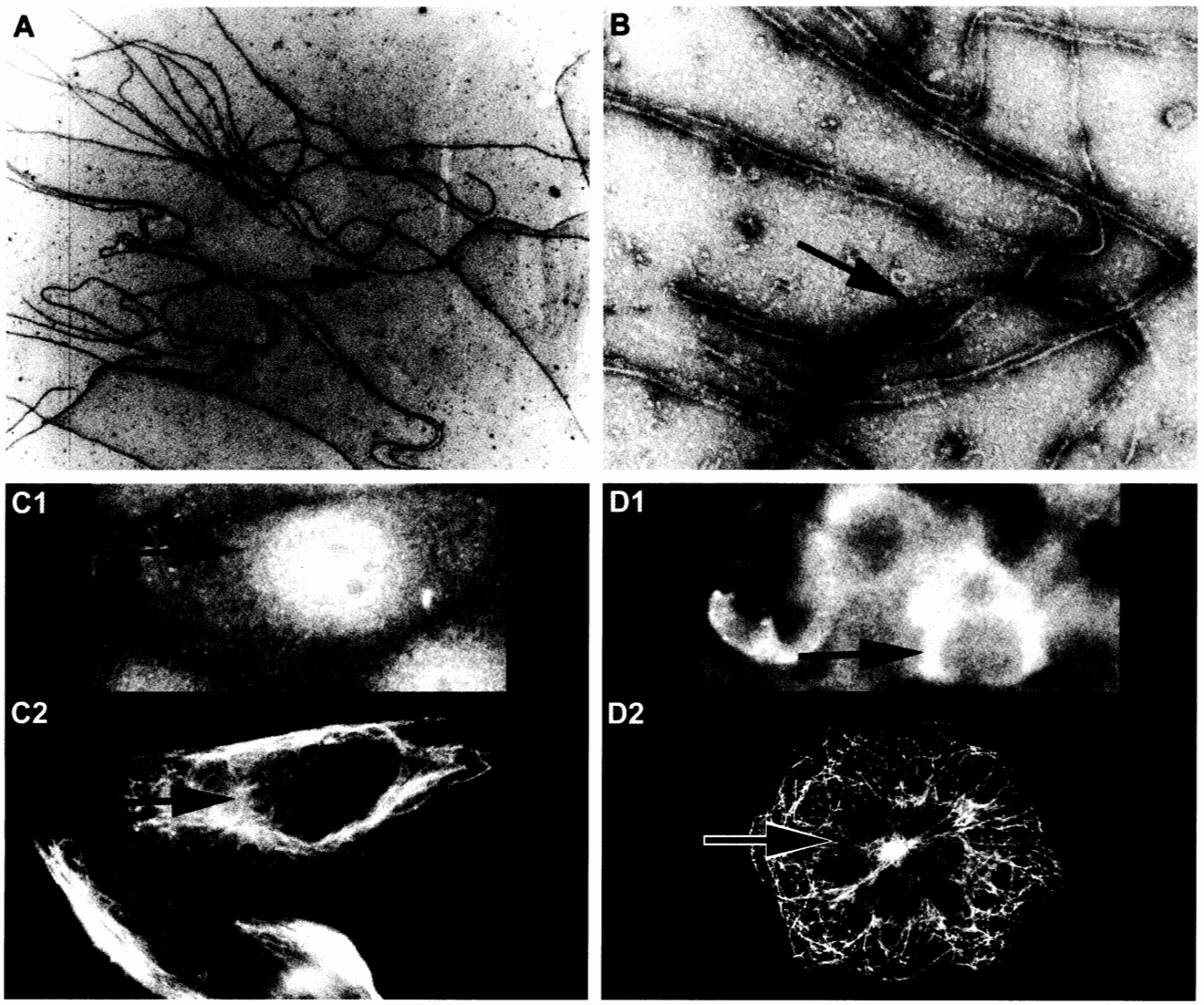


Fig. 5. Alpha-tubulin polymerization is depicted from the single stranded (Panel-A) to the 13-stranded protofilament (Panel-B). Panel-C1 depicts the perinuclear immunofluorescent localization of P149 in an MCF-7 cell (Mizejewski and MacColl, 2003) compared with the known anti-tubulin immunofluorescent-localization (perinuclear) of cytoskeletal tubules in HeLA fibroblast-like tumor cells (C2). Likewise, in Panel-D1, the cytoplasmic localization of P149 in the MCF-7 cell is shown in comparison to the anti-tubular antibody localization in the entire cytoplasm of HELA cells. Electron micrographs were prepared by Professor George Smith with magnifications of: A = 24,000×, B = 156,000×, C2 = 2000×, D2 = 1600×.

locations, it was concluded that the internalized peptide must has been transported from the cell surface through the EPR to the perinuclear region as previously reported for other epithelial cells (Mizejewski, 2001b). A G-coupled receptor on cancer cells that bound to cyclic GIP had been proposed in a previously published study of GIP fluorescence localization (Mizejewski and MacColl, 2003). In view of this previous proposal, the linear GIP might have gained cellular entrance by G-coupled receptor-mediated endocytosis through the plasma membrane. The insulin-like growth factor-1 receptor (IGF-1R), a G-coupled receptor, could be a viable candidate (see below) since the GIP has been shown to display sequence similarity to insulin-like growth factor-associated proteins (Butterstein et al., 2003b).

## 6. Microtubular polymerization

Tubulin, the major protein of microtubules, is a highly polymorphic protein found in a variety of cell types. In conjunction with other elements of the cytoskeleton, microtubules are implicated in various cell functions, including chromosome segregation during mitosis and meiosis, distribution and transport of various organelles, determination of the cell morphology, and cell polarity (Audebert et al., 1993). Thus, microtubules are thought to have structural, organizational, and motility-related functions. Microtubules are protein polymers that form a cytoskeletal rod-like structure composed of 13 protofilaments whose axis runs parallel to that of the microtubule. The protofilaments, in turn, are formed by the head-to-tail association of tubulin dimers. The microtubular cytoskeleton, as structural scaffolding, helps to define and maintain cell shape; as cell organizers, microtubules serve as tracks along which molecular complexes (including ERs) and organelles are transported; and as motility-related structures, microtubules can generate mechanical forces assisted by motor proteins i.e., chromosome segregation during mitosis (Mickey and Howard 1995). While the plasma membrane-associated microtubules regulate receptor mobility and surface distribution, cytoplasm-associated microtubules mediate the endocytic/exocytic process (Thatte et al., 1994).

The microtubular polymerization experiments using GIP were performed using α-tubulin brain extracts from newborn chickens (Rebhun et al., 1974; Weisenberg, 1972). Viscometric measurements with α-tubulin alone (control-1, 25 ng/ml) yielded specific viscosity values which increased gradually during a 30 min incubation period and ranged from 0.10 to 0.40 units (Fig. 6). In comparison, P149 peptide added at varying concentrations displayed a parallel rise with time, correlating with increasing GIP concentrations from 25 ng/ml to

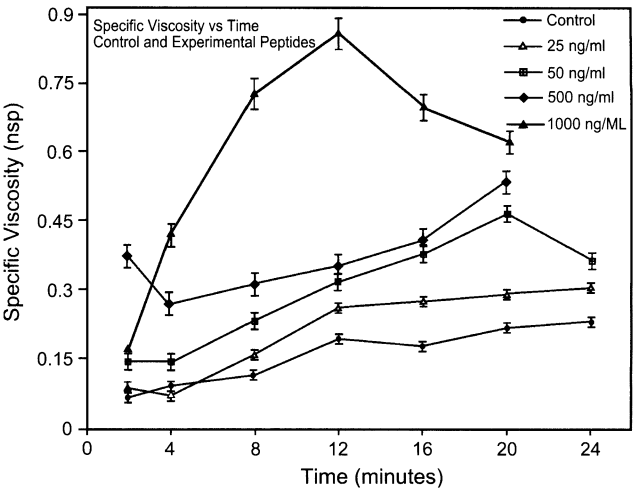


Fig. 6. Microtubular polymerization kinetics were studied using α-tubulin alone (25 ng/ml) versus four increasing concentrations of P149 while retaining constant amounts (25 ng) of α-tubulin. The α-tubulin was obtained from newborn chick brain as previously described (Rebhun et al., 1974). Chick brains were prepared in cold reassembly buffer (RB) which contained 0.1 M Pipes, 1 mM $MgCl_2$/1 mM EGTA/1 mM GTP and pH adjusted to 6.95, and were homogenized and centrifuged at 35,000*g* at 4 °C for 60 min. For analysis of the effect of P149 on dynamic instability, tubulin microtubules were assembled to steady state by adding 25 ng/ml chick brain tubulin (depleted of microtubule-associated proteins) to increasing amounts of P149 (see Fig. 5). The tubulin extract preparations, which were stored in a depolymerized state, were incubated at 37 °C in timed experiments with and without the addition of various P149 peptide concentrations. Note that increasing concentrations of peptide together with a constant amount of tubulin incrementally increases the specific viscosity of the solution up to 1000 ng/ml of peptide, indicating a 4-fold increase in tubulin polymerization.

500 ng/ml. The addition of 1000 ng/ml peptide to the reaction vessel resulted in specific viscosity readings that showed a steep rise and peaked at a 4-fold increase in microtubule polymerization at the 12 min time interval. The specific viscosity reading then declined to a level, at 20 min that still exceeded the rate of polymerization at 500 ng/ml P149 concentration. Thus, the P149 peptide enhanced the ability of α-tubulin to polymerize in a cell-free solution. Other control protein/peptides did not demonstrate this property and behaved similarly to tubulin alone. These data suggest that P149 displays the properties of a microtubule-associated protein. It is of interest that agents such as taxol that enhance tubulin polymerization also promote the endocytotic process of peptide internalization (Thatte et al., 1994).

Previous reports have identified a close association between the ER and the cytoskeletal proteins, tubulin (50–55 kDa) and actin (45 kDa), in uterine and other reproductive tissues (Zafar and Thampan, 1995; Dingwall and Laskey, 1986). Phosphorylation of these proteins is under the regulatory influence of E2 and the cyclic nucleotides, cAMP and cGMP (Baldi et al., 1986). The MER is internalized following E2 binding,

migrates toward and into the nucleus, to interact with DNA-binding proteins (Xu et al., 2004). The movement of the ER toward the nuclear pore complex is facilitated by binding with the cytoskeleton. This association is influenced by the state of phosphorylation of the cytoskeletal molecules. The ERs interaction with the cytoskeletal proteins is further mediated by the heat shock proteins (HSP-90, HSP-70) which chaperone binding of the receptor to the actin filaments (Czar et al., 1996; Scherrer and Pratt, 1992). It has been proposed that the cytoskeletal network that extends between the plasma membrane and the nuclear pore complex forms the network surface (rails) on which the ER receptor complex migrates, via the assistance of motor proteins, toward the nucleus (Fig. 3). Movement along the cytosketelal tracks is dependent on the motor proteins, kinesin and dynein (Hertzer et al., 2003; Bringmann et al., 2004; Yildiz et al., 2004). Kinesin uses the energy of ATP hydrolysis to generate unidirectional processive movement of organelles and complexes along the microtubules (Klumpp et al., 2004).

Extensive networks of microtubules (see Fig. 5) are present in all eukaryotic cells and this trabecular system radiates throughout the cell from a microtubule-organizing center near the nucleus called the centrosome (Oakley, 2000). The centrosome itself is tightly coupled to the nucleus (Gonczy, 2004). Microtubules converge from the cell membrane toward the nucleus, and ultimately to the centrosome where the minus-ends of the microtubules comprising this organelle bind to various tubulins. When fluorescent antibodies to α-tubulin are used (Fig. 5), perinuclear areas of the cell are stained due to the existence of a large pool of soluble tubulin in this region. Furthermore, protein aggregation is more likely to develop in the perinuclear region of the cytoplasm. Perinuclear localization of peptides/proteins occurs as a consequence of their binding to microtubules through an interaction with various members of the tubulin protein family. Peptides/proteins are often detected around the nucleus where they co-localize with this denser part of the microtubular network (Hoffner et al., 2002). The tubulin-binding properties of peptides/proteins could bring peptides like the GIP to the perinuclear region near the centrosome, close to the vicinity of the nuclear pores. It is of interest that the GIP (P149) shows AA-sequence identity (Table 1) to both cytoplasmic and nuclear-associated cytoskeletal proteins and that the GIP was microscopically detected in the perinuclear region (Fig. 4). In addition to plasma membrane scaffolding proteins, another site of signaling protein nucleation is the cytoskeletal contact point with the plasma membrane (see Fig. 5C and D). In this regard, it has been reported that E2 increases levels of ezrin/moesin which function as cytoskeletal linker proteins serving to bridge the actin cytoskeleton to the integral proteins of the plasma membrane (Smith et al., 2002; see sequence matches, Table 1). It is now accepted that estrogen regulates the expression and function of microtubule-associated protein (MAP) complexes (Lamb et al., 1997; Allen et al., 1997). Thus, antiestrogenic compounds (such as GIP) should suppress such estrogen-induced protein expression and function. Stimulation of G-protein coupled receptors also results in a rapid increase in the tyrosine phosphorylation levels of docking proteins such as Shc, (see Fig. 7), tyrosine kinases such as EGF and PDGF, and the Src-2,3 family of non-receptor tyrosine kinases (Davidson et al., 2004).

## 7. Inhibition of ABO antibody-induced erythrocyte agglutination

The assay for erythrocyte agglutination, employing anti-A antiserum incubated with erthyrocytes (RBCs) bearing A-antigens of the ABO system, was employed as previously described (Yamamoto, 2004; Brecher, 2003; Treacy and Stroup, 1987; Linden et al., 1993). The P149 peptide was admixed with A-type RBCs and anti-A antibody serum, diluted in a titration series, and incubated for 30 min. Resultant data indicated that the GIP at 150 μg/ml and 600 μg/ml, inhibited RBC agglutination over a range encompassing 3–5 2-fold serial dilutions greater than control tubes. As displayed in Table 4, the serial 2-fold dilutions of the anti-A antiserum together with 150 μg P149 effected RBC agglutination inhibition starting at 1:32 antibody dilution and endpointing at a 1:128 dilution. Control tubes did not display an endpoint until 1:512. In contrast, when the antibody/RBC mixture was exposed to higher GIP concentration (600 μg), agglutination inhibition occurred at 1:4 dilution and extended to the 1:32 dilution of the antibody. In comparison, the control tubes in the experiment achieved endpoint at 1:512 dilution. It is apparent that the incubation of the GIP with A-antigen bearing RBCs and anti-A antibodies inhibited the hemagglutination reaction on the RBC cell surface.

The cytoskeletetal matrix stemming from the erythrocyte membrane consists of four major protein compounds, namely, spectrin, actin, glycophorin, and ankyrin (Batrukova et al., 2000; Zail, 1986; Palek 1981). Since receptors, such as the ER, have been shown to exist as part of this microtrabecular network of the cytoplasmic RBC cytoskeleleton, erythyrocyte "ghost" preparations have been employed to study isolated-membrane receptors (Sterling et al., 2004). Such studies have provided evidence to show that a limited number of these high-affinity MERs ($10^{-9}$ M) co-localize on the cytoplasmic interface of the plasma membrane with microtubule components of the RBC cytosketelal matrix (Puca and Sica, 1981). Various types of the ER including the E2-activated form, bind with

high affinity to the cytoskeleton, especially in cation-supplemented environments. Thus, studies have already provided evidence that the ER interacts with high binding affinity and in a specific and saturable manner with components of the erythyrocyte cytoskeletal system, and that cations can modify the outcome of the uterine growth assay (Table 2).

Regarding the ABO erythrocyte agglutination inhibition by the P149 peptide, the intact full-length AFP molecule has also previously been shown to inhibit ABO antibody-induced erythrocyte agglutination (Brenner et al., 1985; Lubetzki-Korn et al., 1984). The ABO blood group on the surface of erythrocytes RBCs induces the formation of naturally occurring antibodies in the human blood circulation. The plasma membrane of the RBC consists of a bilipid/protein structure from which protrudes a myriad of proteins including glycoproteins, lipoproteins, and other proteinaceous hetero-conjugates (Rice-Evans and Chapman, 1981). Glycophorin (MN blood group) and ankyrin constitute intergral transmembrane proteins of the RBC-glycocalyx which forms the infrastructure of the RBC plasma membrane (Zhang and Kiechle, 2004). Glycophorin serves to prevent RBC aggregation and/or agglutination. Thus, proteins or peptides that bind to the RBC surface could sterically interfere with or obstruct antigen-antibody reactions at the cell surface. The GIP, incubated with A-antigen bearing RBCs and anti-A antibodies, inhibited RBC agglutination over five 2-fold serial dilutions over that of control tubes. It is tempting to speculate that the GIP was bound and docked to an integral membrane receptor near the MER which was tethered to the inner surface of the RBC plasma membrane. It is of further interest that a genebank search indicated that an AA stretch on the GIP matched an identity/similarity segment on the glycophorin and ankyrin molecules, which are integral cell-surface proteins within the RBC membrane (see above). The ankyrin repeat is a ubiquitous 33 AA residue protein-to-protein interaction motif on proteins that adopt a β-hairpin helix-loop-helix fold (Batrukova et al., 2000; Bennett et al., 1985). The P149A fragment provided the best match to the glycophorin-A isotype, while ankyrin repeat segments matched to both the P149b and the P149c segments.

## 8. Changes in cell morphology

Astroglial cell cultures prepared from four different brain regions cerebellum, hippocampus, cortex, brain stem, were dissected from 3-day-old rat pups (Gennuso et al., 2004; Chen et al., 2000). When these cultures were approximately 50% confluent the cells were treated with varying concentrations of P149 peptide. Astroglial shape change was elicited by the GIP in three of the four brain regions. No response was observed from astroglial cells derived from the brain stem. The largest number of cells responding to the GIP was observed in the hippocampal cultures, intermediate cell numbers responded in the cerebellum; and while the fewest cells responded in cortical cultures (see Table 5). Dose-dependent responses were observed in cerebellar, hippocampal, and cortical cultures; the respective $EC_{50}$ values calculated for these responses were 30, 3, and 3 nM.

The glia cells, even though they are nine times as abundant as neurons, were once thought to have only a maintenance role in the brain. That is, glia were only supposed to provide nutrients, ions, protection, and interstitial support to the neurons. However, it has recently been reported that astroglial cells can generate an action potential by means of chemical rather than electrochemical signals (Stevens et al., 2002) The chemical signal initiates an influx of calcium ions in the glial cells by opening a voltage-sensitive ion channel and raising the concentration of calcium in the cells' own cytoplasm. Neurotransmitters (e.g. glutamate) and other hormonal stimulations of the astroglia (Sato et al., 2003) but not Schwann cells or oligo-dendrocytes, release adenosine triphosphate (ATP) to their surroundings, which bind to receptors on nearby astrocytes (Fields and Stevens-Graham, 2002; Sato et al., 2003).

Table 4
Growth inhibitory peptide (P149) inhibition of anti-A antibody-induced human erythrocyte agglutination using 2-fold antiserum dilutions[a]

| | Anti-A dilution | | | | | | | | | | | |
|---|---|---|---|---|---|---|---|---|---|---|---|---|
| | 1:1 | 1:2 | 1:4 | 1:8 | 1:16 | 1:32 | 1:64 | 1:128 | 1:256 | 1:512 | 1:1024 | 1:2048 |
| P149 (600 μg) | 4+ | 4+ | 3+ | 2+ | 1+ | 0 | 0 | 0 | 0 | 0 | 0 | 0 |
| P149 (150 μg) | 4+ | 4+ | 4+ | 4+ | 3+ | 2+ | 1+ | 0 | 0 | 0 | 0 | 0 |
| Saline control | 4+ | 4+ | 4+ | 4+ | 4+ | 4+ | 3+ | 2+ | 1+ | ± | 0 | 0 |

[a] The erythrocyte agglutination assay employed a 2-fold diluted titration of anti-A antiserum incubated together with erythrocytes (4% cell suspension) bearing A-antigens of ABO system. A suspension of either 150 μl or 600 μl of P149 peptide (1.0 mg/ml) together with 50 μl of anti-A serum (Ortho Diagnostics, Raritan, NJ) was pre-incubated for 30 min at room temperature. Following the pre-incubation (equilibration), 50 μl of A-antigen bearing erythrocytes were added to each tube, gently mixed, and incubated for another 30 min at ambient temperature. At the end of this time interval, the reaction tubes were centrifuged (low speed), and results were read, and recorded. Reactions were read microscopically for each 2-fold titration until at least two consecutive negative (zero) endpoints were observed. Control tubes were handled in the same fashion, except that saline was substituted for the peptide solution. Other control substances (peptides) showing less than a two dilution difference from zero were not considered significant. Se references: Treacy and Stroup (1987), Linden et al. (1993) and Brecher (2003).

Once ATP is bound, it prompts ion channels to open setting up a chain reaction of calcium ion responses across the population of astrocytes. The signal influx travels from the cell membrane to the nucleus, causing various genes to switch on (Sul et al., 2004). Thus, the receptors on the astroglia cells (with ligands such as ATP, neurotransmitters, adenosine) can respond to induce immediate cell shape and polarity changes.

The change in cell shape in astroglial cells exposed to GIP further supports the above contention that cytoskeletal interactions are a downstream consequence of peptide interaction of the GIP at the cell surface. Astroglial cells may modulate neural signals by physically altering their extracellular occupied space adjacent to neurons in the central nervous system. Such changes have been studied in detail in hypothalamic nuclei, where large populations of astroglia change their morphology following hormonal (e.g. E2) signal stimulations (Galbiati et al., 2003; Melcangi et al., 2002). Such changes may be responsible for increased neuronal excitability as discussed above. It is clear that subpopulations of astroglia from other brain regions undergo similar changes in cell culture. The change in astroglial morphology can be mediated by activation of specific neurotransmitter and/or hormone receptors which are in turn coupled to cyclic-AMP and phosphoinositide and are responsible for these signal transduction pathways (Galbiati et al., 2003). The experiments, designed to determine whether astroglia change their morphology following exposure to the GIP, demonstrated that phenomenon. Thus, observed cellular change shape appears to represent a consequence of GIP-to-plasma membrane interaction which may affect the cytoskeleton. This conclusion is further supported by the genebank sequence matches (Table 1) of GIP to both ezrin and moesin, which represent a family of proteins that function in the maintenance of cell shape and lamellipodial extension (Lamb et al., 1997).

Table 5
Summary of rat brain astroglial shape change response to the alpha-fetoprotein-derived growth inhibitory peptide (P149)[a]

| Tissue source of astrocytes | $EC_{50}$ (nM) | Maximum cells responding (% of total) |
|---|---|---|
| Cerebellum | 30 | 23 |
| Hippocampus | 3 | 42 |
| Cortex | 3 | 9 |
| Brain stem | No response | No response (<1–3%) |

[a] Astroglial cell cultures dissected from four different brain regions (cerebellum, hippocampus, cortex, brain stem) were obtained from 3-day-old rat pups. When the cultures were approximately 50% confluent, cells were treated with varying concentrations of P149 peptide. After 1-h incubation, cells were fixed and their morphology was analyzed using phase optics. At least 100 cells were counted in three different fields on each coverslip. Cells were scored positive for shape change if they contained a cell process that was ≥ the diameter of the cell soma. Data were presented as % of cells changing shape. Dose-dependent effects were determined at least three times for astroglia from each brain region. Control substances (peptide, proteins) showing (<1–3%) cell shape changes were not considered significant. See references: Davis-Cox et al. (1994), Shain et al. (1992) and Kam et al. (2002).

## 9. Dye and fluorescent binding assays

Both the GIP and the P149b segment were subjected to UV/vis spectrophotometric assays of fluorescent and hydrophobic dye binding, respectively (Kindu and Guptasarma, 1999; Kim et al., 2003). When these peptides in phosphate buffered saline were assayed using Congo Red (CR), an upward spectrophotometric shift peaking at 510–552 nm was observed with P149b, while the P149 spectra were identical to that of Congo Red alone (Table 6 and Fig. 7A). Absorption spectra showed that the peptide P149b shifted the absorbance maximum of Congo Red from 485 nm to 505 nm. The

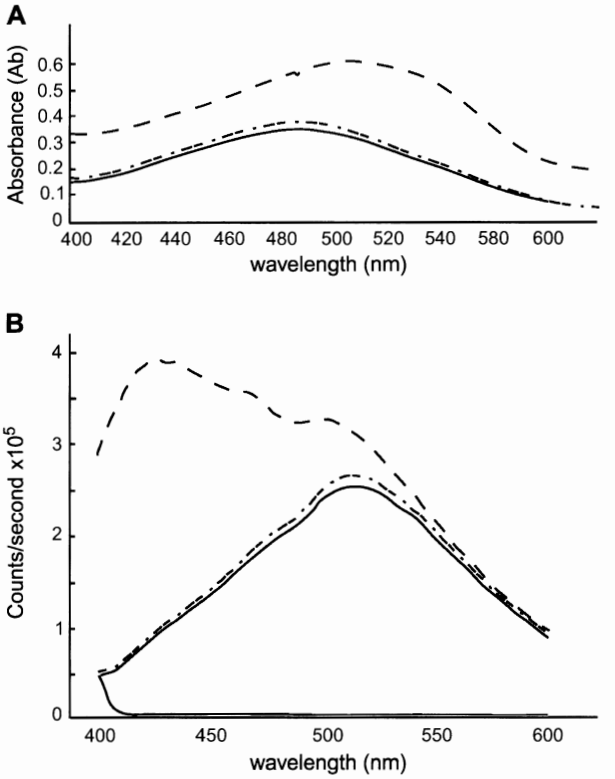


Fig. 7. Spectrophotometric assays of Congo Red hydrophobic dye (Panel-A) and ANS fluorescent binding (Panel-B) of P149 and P149c are illustrated. Peptides P149 and P232 were prepared in 0.1 M Tris, pH 9 at 5 mg/ml. Congo Red was prepared at 20 μM in PBS at pH 7.4. Solutions for spectroscopy were prepared by mixing 40 μl of peptide with 960 μl of Congo Red solution and then incubating at room temperature for 30 min. Absorption spectra 400–600 nm were collected on an HP8453 diode array spectrophotometer in 1 cm pathlength cuvets. Fluorescence emission spectra were collected on a PT1 Quantamaster fluorometer using a wavelength from 400 nm to 600 nm with an excitation wavelength of 375 nm. See text for assay results and reference. ANS = 8 anilinonapthalene-sulfonic acid. - - - - = P149b; · - - · = P149; ——— = dye alone.

Table 6
Growth inhibitory peptide (P149) interaction with and/or binding to various ligands, enzymes, and organic/inorganic agents

| Interacting or binding agent | Growth inhibitory peptides | | | | |
|---|---|---|---|---|---|
| | P149 | P149a | P149b | P149c | References |
| (1) Human estrogen receptor (HER) (recombinant) | Binding | Binding | Non-binding | Non-binding | Vakharia and Mizejewski, 2000; Richardson, 1999 |
| (2) 17β-Estradiol | Non-binding | Non-binding | Binding | Non-binding | |
| (3) Diethystilbesterol in the uterine assay | Inhibits uterine growth (36%) | Not tested | Not tested | Not tested | Mizejewski, 1998, 2003 |
| (4) Human chorionic gonadotrophin (ovarian stimulation) | Inhibits ovarian growth (33%) | Not tested | Not tested | Not tested | Mizejewski, 1998; Mizejewski and MacColl, 2003 |
| (5) Human insulin[a] (recombinant) teratogenic doses | Reduces birth defects (50%); reduces growth (65%) | Not tested | Not tested | Not tested | Butterstein et al., 2003a |
| (6) 17 β-Estradiol[b] fetotoxic doses | Reduces fetotoxic effect (73%) | Reduces fetotoxic effect (63%) | Reduces fetotoxic effect (67%) | Reduces fetotoxic effect (37%) | Butterstein et al., 2003a |
| (7) Thyroid hormone[c]-induced metamorphosis | Inhibit tail resorption (66%) | Not tested | Not tested | Not tested | Butterstein and Mizejewski, 1999; Jacobson, et al., 1999 |
| (8) Tissue factor esterase enzyme | Inhibits thrombin induction (33%) | Not tested | Not tested | Not tested | Mizejewski et al., 1996; Ohashi et al., 2003; Henrikson et al., 1990 |
| (9) Immature mouse uterine (E2 induced) | Inhibits uterine growth (39%) | Inhibit uterine growth (28%) | Inhibit uterine growth (22%) | Inhibit uterine growth (42%) | Mizejewski et al., 1986; Vakharia and Mizejewski, 2000 |
| (10) Acetylcholinesterase (soluable enzyme) | Inhibits enzyme activity (40%) | Not tested | Not tested | Not tested | Lasner et al., 1995; Wang and |
| (11) Acetylcholinesterase (cell bound enzyme)[d] | Enhances enzyme activity (35%) | Not tested | Not tested | Not tested | Chen, 1992 |
| (12) P450 aromatase (microsomal enzyme) | Inhibits enzyme activity (35%) | Not tested | Not tested | Not tested | Fasco et al., 1977; Zhang et al., 1995 Mizejewski, 2001a,b |
| (13) Hydrophobic dyes | | | | | |
| (a) Congo Red | Non-binding | Not tested | Binding | Not tested | |
| (b) ANS fluorescent dye | Non-binding | Not tested | Binding | Not tested | |
| (14) Heavy metals: cobalt, zinc, copper | Binding with all cations | Non-Binding. CYS → ALA. mutation | Binding, HIS → ALA, mutation | Non-binding | MacColl et al., 2001; Butterstein et al., 2003a |

ANS = anilinonapthalene-sulfonic acid. (12) = Rat liver microsomal fraction.
[a] Insulin-induced teratogenic doses in the fetal chick.
[b] Estrogen-induced fetotoxic doses in the perinatal mouse.
[c] Amphibian tadpole metamorphosis.
[d] Torpedo electric eel enzyme.

34-mer GIP had no effect on the absorption when its spectrum was compared to that of the control Congo Red solution. Again, using fluorescence spectroscopy with 8-anilinonapthalene-sulfonic acid (ANS) binding to the peptides, only P149b displayed an upward spectral shift while the P149 peptide showed no effect (Table 6 and Fig. 7B). That is, in the presence of ANS, solutions of peptide P149 showed fluorescence emission spectra essentially identical to control ANS solutions, with a peak around 500 nm. However, P149b showed emissions with peaks at 420 nm and 470 nm, which are not normally characteristic of ANS, in addition to the 500 nm peak. Since ANS binding occurs on protein/peptides in the unfolded state, it would seem that the trimer and/or dimer configuration of P149 sterically hinders complexing of ANS with the 34-mer GIP. In reference to Congo Red, the same reasoning would likewise reflect hindrance to hydrophobic dye binding. In comparison, binding of the GIP to cobalt and zinc (MacColl et al., 2001; Butterstein et al., 2003a) suggested that a distorted tetrahedral symmetry of the peptide–metal interface formed by the cysteine/histidine residues was still available for complex formation (Table 6). The zinc–GIP complex was shown to display antigrowth activity and did not form the intrapeptide (dimer) disulfide bond characteristic of the free GIP in aqueous solution. It is interesting that when the P149b segment was bioassayed in the immature rat, a 38% inhibition of E2-stimulated growth was observed; in comparison, when $Zn^{++}$ was complexed to the peptide,

the growth inhibitory potency was not only similar to unliganded GIP, but actually enhanced the activity. Thus, metal-complexing to P149 does not impede uterine growth inhibition and appeared to slightly enhance it (Butterstein et al., 2003a). As shown in Table 6, P149 and its segments interact with a variety of ligands, hormones, enzymes, and growth factors as previously reported (see references in table).

Hydrophobic amino acids are usually tucked into the inner core of a protein or a peptide. When a protein folds into its native tertiary structure, it forms a compact molecular complex with its hydrophilic charges projecting outward, and its hydrophobic charges (derived from its amino acids) directed inward (Mizejewski, 2001a,b; Uversky et al., 1995, 1997a,b). When a protein unfolds, the hydrophobically charged-amino acids are exposed and are available for binding to hydrophobic dyes. Two such hydrophobic dyes used in protein folding experiments were CR and ANS. Congo Red emits light at a wavelength of 485 nm while ANS is a fluorescent dye emitting at a wavelength of 500 nm. Using methods of both light and fluorescent spectroscopy, it was shown that the 14-mer middle segment of GIP (P149b) binds both dyes. The importance of CR lies in its published use of binding to beta-amyloid fibers found in Alzheimer's patients (Yong-Sung et al., 2003; Kim et al., 2003). The binding of peptides/protein to the fluorescent dye, ANS, has been used as a biochemical tool in which to study the unfolding of HAFP to the molten globular state (Uversky et al., 1997a,b). Perhaps the GIP region is involved in folding/unfolding of the native AFP protein itself. Finally, in light of hydrophobic binding to P149b it should be possible to individually bind both of these dyes to the entire 34-mer GIP in its linear configuration. This could be done by methylating the cysteine amino acid only in the first 12-amino acid segment of the 34-mer peptide. By methylation or amidation, the 34-mer GIP should not form a dimer-like (cyclic) peptide via a disulfide-bridge with the cysteines on the mid-piece. Hence, the GIP should remain a linear peptide that has the middle 14 AAs still available for dye binding. This strategy has already been employed to bind heavy metals to beta-amyloid peptides (Dong et al., 2003).

In reference to the hot-spot discussed in Section 1 of this review, it was proposed that stress/shock conditions in the fetal milieu (e.g., high E2 levels) could induce a conformational change in HAFP. It is tempting to speculate that the P149b segment, which binds hydrophobic ligands, is the hot-spot of the GIP amino acid stretch on native HAFP. It is also germane to this discussion that a phosphorylation site could potentially be located at either side of the P149b segment (amino-terminal = Ser AA #2; carboxyterminal = Thr AA #29) lying within the 34-mer peptide. These potential Src-3 (Ser/Thr kinases) phosphorylation sites could provide the necessary energy to initiate the conformational change that needs to occur following ligand binding, as reported for other proteins (Uversky et al., 1997a,b) The phosphorylation-dependent conformational change is induced by the peptidyl–prolyl *cis/trans* isomerase enzyme which isomerizes only the ser/thr-pro AA motif, such as present on P149c (Lu et al., 2000; Lu, 2004). In a manner to binding estradiol by P149b, it may potentially produce a conformational change similar to that seen with HAFP complexed with E2. In this fashion, the exposure of the GIP site on the HAFP molecule may be induced by one of a variety of ligands that bind to the hydrophobic core of the P149b segment (e.g., E2, fatty acids, dyes, metals, Table 6). The purified 15 AA hydrophobic mid-piece (P149b) resembles the 15 AA-helix structure observed in anti-bacterial peptides which display a 3 residue repeat periodicity of hydrophobic AAs (III), hydrophobic AAs (LCI) and hydrophilic (RHE) AA residues (Tew et al., 2002).

## 10. Mechanism of action

In view of the data summarized in this review, a mechanism of action may be proposed for the estrogen-sensitive growth regulatory effects observed for GIP. Following administration in vivo, E2 serves as a growth-promoting agent in immature tissues such as the uterus, or in transformed E2-dependent breast cancer cells (Mizejewski and MacColl, 2003; Migliaccio et al., 2003). Likewise, administration of the GIP results in homing of this peptide to tissue areas of up-regulated growth, as seen in estrogen-targeted cells 24 h later (Fig. 3). By means of receptor-mediated endocytosis via integral cell membrane proteins, the GIP might gain access through the plasma membrane while encountering the membrane-associated caveolae (Parton, 2003). Since the ER has been reported to localize to the inner membrane portion of the caveolae, it is conceivable that the GIP binds to the membrane-tethered ER, a peptide-to-ER binding interaction that has been demonstrated in vitro (Vakharia and Mizejewski, 2000).

It has recently been shown that ER$\alpha$, soon after translation on the ribosomes, translocates to the plasma membrane caveolae and resides there, attached as a complex with the SHc adaptor/scaffold protein (Fig. 8) (Song et al., 2004). The caveolae/lipid rafts have been shown to be essential for insulin-like growth factor-1 receptor (IFG-1R) signaling during the induction of cell activation, proliferation, and differentiation (Glebov and Nichols, 2004). The IGF-1 receptors were reportedly located in caveolar plasma membranes and are intimately involved in signal transduction cascades (Song et al., 2004). Binding of the GIP to the ER could involve the steroid receptor segment region that recognizes the co-activator NR-box (see Fig. 1,

plasma membrane of uterine cells without interacting with the membrane-bound estrogen receptor, one could propose that linear P149 could serve as an intracytoplasmic decoy binding protein and indirectly disrupts the uterine cells' physiological biphasic response to estrogen stimulation. In any event, GIP is translocated to the perinuclear region of the cell (Fig. 4), regardless of which mechanism is involved. Therefore, GIP produces growth arrest either as a cell-surface event or as an intracytoplasmic effector agent.

## 11. Concluding remarks

In the course of this review, it has been demonstrated that the growth inhibitory motif on HAFP serves a role in both estrogen-sensitive growth and in cytoskeleton-associated functions. The AFP-derived 34-mer GIP and its three subsegments have been studied in the suppression of ontogenetic growth in the immature rodent growth assay under pre-incubation conditions involving a variety of cations, ligands, and amino acid mutations. Furthermore, the GIP and each of its segments differ in their abilities to bind various receptors, dyes, and heavy metals. Thus, the AFP-derived peptides are potential candidates in the study of embryonic and fetal developmental processes such as differentiation events including thyroid-induced amphibian metamorphosis, onset of puberty, and vertebrate organ/tissue regeneration models. Because the peptides act on a multitude of proliferating, differentiating, and regenerating tissues, the GIP and its segments could be used to seek out and identify molecular targets and to deliver conjugated or bound cargoes to the interior of cells. The peptides might also serve in studies of such phenomenon as receptor blockage and/or signal blunting, cell penetration, inhibition of protein-to-protein cascade interaction, and antagonism of intracellular trancytosis. Small organic non-peptide mimics could also be modeled to the P149 peptide, to provide second-generation inhibitor molecules. Thus, AFP-derived peptides could potentially find utility in the identification of molecular targets for lead compounds in drug discovery of "biological response modifiers" for various human diseases and disorders.

## Acknowledgements

We thank Dr. James Dias, Dr. Charles Hauer, Dr. Angelo Lobo, Dr. Li-Ming Changchien, Dr. Robert MacColl, James Seeger, and Leslie Eisele of the Peptide Synthesis, Mass Spectroscopy, and Biochemistry Core Facilities of the Wadsworth Center for the expert preparations, characterization, purification, and analysis of the peptides. Gratitude is also extended to Drs. William Shain and Jeanne Linden of the Wadsworth Center and Dr. Kristen Fox of Union College for their research collaboration. The authors also wish to express their sincerest thanks and deepest gratitude to our previously published manuscript co-authors and to Lynda M. Jury for her commitment and time expenditure in the excellent typing and processing of the manuscript, references, and tables of this report.

## References

Abelev GI. Alpha-fetoprotein in association with malignant tumors. Adv Cancer Res 1971;14:295–317.

Acconcia F, Bocedi A, Ascenzi P, Marino M. Does palmitoylation target estrogen receptors to plasma membrane caveolae? Life 2003;55:33–5.

Allen DL, Mitchner NA, Uveges TE, Nephew KP, Khan S, Ben-Johathan N. Cell specific induction of c-fos expression in the pituitary gland by estrogen. Endocrinolology 1997;138:2128–35.

Allen SHG, Bennett JA, Mizejewski GJ, Andersen TT, Ferraris, Jaccobson HI. Purification of alpa-fetoprotein from human cord serum with antiestrogenic activity. Biochem Biophys Acta 1993; 1202:135–42.

Audebert S, Desbruyers E, Koulakoff A. Reversible polyglutamation of α-and β-tubulin and microtubule dynamics in mouse brain neurons. Mol Biol Cell 1993;4:615–26.

Baldi A, Boyle DM, Wittliff JL. Estrogen receptor is associated with protein and prospholipid kinase activities. Biochem Biophys Res Commun 1986;135:597–606.

Batrukova MA, Betin VL, Rubtsov AM, Lopina OD. Structure, properties and functions. Biochemistry (Moscow) 2000;65:469–84.

Bennett JA, Mizejewski GJ, Allen SHG, Zhu SJ, Jacobson HI. Transformation of alpha-fetoprotein to a negative regulator of estrogen-dependent growth by ligands of the steroid/thyroid hormone receptor superfamily. 18th International Congress. J Cancer Res Clin Oncol 1993;34:244.

Bennett JA, Semeniuk DJ, Jacobson HI, Murgita RA. Similarity between natural and recombinant human AFP as inhibitors of estrogen-dependent breast cancer growth. Breast Cancer Res Treat 1997;45:169–79.

Bennett V, Baines AJ, Davis JQ. Ankyrin and synapsin:spectrin-binding proteins associated with brain membranes. J Cell Biochem 1985;29:157–69.

Bramlett KS, Burns TP. Effect of selective estrogen receptor modulators (SERMS) on coactivator nuclear receptor (NR) box binding to estrogen receptors. Mol Genet Metab 2002;76: 225–33.

Bramlett KS, Wu Y, Burns TP. Ligands specify coactivator nuclear receptor (NR) box affinity for estrogen receptor subtypes. Mol Endocrinol 2001;15:902–22.

Brecher M. Technical manual. 14 Bethesda, MD: American Association of Blood Banks; 2003. p. 30–40.

Brenner T, Stuff-DeCosta Y, Sicic C, Abramsky O. Inhibition of alpha-fetoprotein fractions of hemagglutination reactions between A and B antigens of human RBC and specific antisera. Clin Immunol Immunopathol 1985;34:2–26.

Bringmann H, Skiniotis G, Spilker A, Kandels-Lewis S, Vernos I, Surrey T. A kinesin-like motor inhibits microtubule dynamic instability. Science 2004;303:1519–21.

Brock DJH, Sutcliffe RG. Alpha-fetoprotein in the antenatal diagnosis of anencephaly and spina bifida. Lancet 1972;2:194–7.

Butterstein G, MacColl R, Mizejewski GJ, Eisele LE, Meservey J. Biophysical studies and anti-growth activities of a peptide, a certain analog, and a fragment peptide derived from AFP. J Pept Res 2003a;61:1–6.

Butterstein GM, Mizejewski GJ. Alpha-fetoprotein inhibits frog metamorphosis: implications for protein motif conservation. Comp Biochem Physiol 1999;124A:39–45.

Butterstein GM, Morrison J, Mizejewski GJ. Effect of alpha-fetoprotein and derived peptides on insulin-and estrogen-induced fetotoxicity. Fetal Diagn Ther 2003b;125:1080–9.

Chen SH, Liu SH, Liang YC, Sy LS. Death signaling pathway induced by pyrolidine dithiocarbmate copper complex in cultured rat corical astrocytes. Glia 2000;31:249–61.

Cheng G, Weihua Z, Warner M, Gustafsson JA. Estrogen receptors ERα and ERβ in proliferation in the rodent mammary gland. Proc Natl Acad U S A 2004;101:3739–46.

Couett J, Li S, Okamoto T, Ikezu T, Lisanti MP. Identification of peptide and protein ligands for the caveolin-scaffolding domain. Implications for the interaction of caveolin with caveolae-associated proteins. J Biol Chem 1997;272:6525–33.

Czar MJ, Welsh MJ, Pratt WB. Immunoflurescence localization of the 90-kDa heat-shock protein to cytoskeleton. Eur J Cell Biol 1996;70: 322–30.

Dauphinee MJ, Mizejewski GJ. Human alpha-fetoprotein contains potential heterodimerization motifs capable of interaction with nuclear receptors and transcription/growth factors. Med Hypotheses 2002;58:453–61.

Davidson L, Pawson AJ, Millar RP, Maudsley S. Cytoskeletal reorganization dependence of signaling by the gonadotropin-releasing hormone receptor. J Biol Chem 2004;279:1980–93.

Davis-Cox MI, Turner JN, Szarowski D, Shain W. Probal ester-stimulated stellation in primary cultures of astrocytes from different brain regions. Microsc Res Tech 1994;29:319–27.

Dingwall C, Laskey R. Protein import into the nucleus. Ann Rev Cell Biol 1986;2:367–90.

Dong J, Atwood CS, Anderson VE, Siedlak SL, Smith MA, Perry G, et al. Metal binding and oxidation of amyloid-β within isolated senile plaque cores: Raman microscopic evidence. Biochemistry 2003;42:2768–73.

Eisele LE, Mesfin FB, Bennett JA, Andersen TT, Jacobson HI, Soldwedel H, et al. Studies on a growth-inhibitory peptide derived from alpha-fetoprotein and some analogs. J Pept Res 2001a;57: 29–38.

Eisele LE, Mesfin FB, Bennett JA, Andersen TT, Jacobson HI, Vakharia DD, et al. Studies on analogs of a peptide derived from alpha-fetoprotein having anti-growth properties. J Pept Res 2001b; 57:539–46.

Engelman JA, Zhang X, Galbiati F, Volonte D, Sotgia F, Pestell RG, et al. Molecular genetics of the caveolin gene family: implications for human cancers, diabetes, Alzheimer disease, and muscular dystrophy. Am J Hum Genet 1998;63:1578–87.

Fasco MJ, Piper LJ, Kiminsky LS. Biochemical applications of a quantitative high pressure liquid chromatographic assay of warfarin and its metabolites. J Chromatogr A 1977;131: 365–73.

Fields RD, Stevens-Graham B. New insights into neuron-glia communication. Science 2002;298:556–62.

Fujimoto LM, Roth R, Heuser JE, Schmid SL. Actin assembly plays a variable, but not obiligatory role in receptor-mediated endocytosis in mammalian cells. Traffic 2000;1:161–71.

Galbiati M, Martini L, Melcangi RC. Role of glial cyst, growth factors, and steroid hormones in the control of LHRH-secreting neurons. Domest Anim Endocrinol 2003;25:101–8.

Gee AC, Carlson KE, Martini PGV, Katzenellenbogen BS, Katzenellenbogen JA. Coactivator peptides have a differential stabilizing effect on the binding of estrogens and antiestrogens with the estrogen receptor. Mol Endocrinol 1999;13:1912–23.

Geistlinger TR, McReynolds AC, Guy RK. Ligand-selective inhibition of the interaction of steroid receptor coactivators and estrogen receptor isoforms. Chem Biol 2004;11:273–81.

Gennuso F, Fernetti C, Tirolo C, Testa N, L'Episcopo F, Caniglia S, et al. Bilirubin protects astrocytes from its own toxicity by inducing up-regulation and translocation of multidrug resistance-associated protein 1 (Mrp1). Proc Natl Acad Sci 2004;101: 2470–5.

Glebov OO, Nichols BJ. Lipid raft proteins have a random distribution during localized activation of the T-cell receptor. Nat Cell Biol 2004;6.

Gonczy P. Centrosomes. Hooked on the nucleus. Curr Biol 2004;14: R268–70.

Haourigui M, Thobie N, Martin ME, Benassayag C, Nunez EA. In vivo transient rise in plasma free fatty acids alters the functional properties of α-fetoprotein. Biochim Biophys Acta 1992;1125: 157–65.

Heery DM, Kalkhoven E, Hoare S, Parker MG. A signature motif in transcriptional co-activators mediates binding to nuclear receptors. Nature 1997;387:733–6.

Henrikson KP, Jazin EE, Greenwood JA, Dickerman HW. Estrogen regulation of a tissue factor-like procoagulant in the immature rat uterus. Endocrinology 1990;126:167–75.

Hertzer KM, McClung SCE, Walczak CE. Kin I kinesins: insights into the mechanism of depolymerization. Crit Rev Biochem Mol Biol 2003;38:453–69.

Hewitt SC, Droo BJ, Hansen K, Collins J, Grissom S, Afshari CA, et al. Estrogen receptor-dependent genomic responses in the uterus mirror the biphasic physiological response to estrogen. Mol Endocrinol 2003;17:2070–83.

Hoffner G, Kahlem P, Djian P. Perinuclear localization of huntingtin as a consequence of its binding to microtubules through an interaction with β-tubulin:relevance to Huntington's disease. J Cell Sci 2002;115:941–8.

Huo H, Guo X, Hong S, Jiang M, Liu X, Liao K. Lipid rafts/caveolae are essential for insulin-like growth factor-1 receptor signaling during #T3-L1 preadipocyte differentiation induction. J Biol Chem 2003;278:11561–9.

Jacobson HI, Andersen TT, Mizejewski GJ, Butterstein G, Mesfin FB, Zhu S, et al. Alpha-fetoprotein inhibits cellular response to estrogen, androgen, glucocorticoid, and thyroid hormone. It is a receptor superfamily inhibitor? Proceedings of the steroid receptor superfamily. Indian Wells, CA; Jan. 8–12, 1999.

Kam L, Shain W, Turner JN, Bizios R. Selective adhesion of astrocytes to surfaces modified with immobilized peptides. Biomaterials 2002;23:511–5.

Kim YS, Randolph TW, Manning MC, Stevens FJ, Carpenter JF. Congo red populates partially unfolded states of amyloidogenic protein to enhance aggregation and amyloid fibril formation. J Biol Chem 2003;10842–50.

Kindu B, Guptasarma P. Hydrophobic dye inhibits aggregation of molten carbonic anhydrose during thermal unfolding and refolding. Prot Struct Gen 1999;37:321–4.

Klumpp LM, Brendza KM, Gatial JE, Hoenger A, Saxton WM, Gilbert SP. Microtubule-kinesin interface mutants reveal a site critical for communication. Biochemistry 2004;43:2792–803.

Lamb RE, Ozanne BW, Roy C, McGarry L, Stipp C, Mangeat P, et al. Essential function os ezrin in the maintenance of cell shape and lamellipodial extension in fibroblast. Curr Biol 1997;7: 682–8.

Lasner M, Roth LG, Chen CH. Structure-functional effects of a series of alcohols on acetylcholinesterase-associated membrane vesicles: elucidation of factors contributing to the alcohol action. Arch Biochem Biophys 1995;317:391–6.

Le PU, Nabi IR. Distinct caveolae-mediated endocytotic pathways target the Galgi apparatus and the endoplasmic reticulum. J Cell Sci 2003;116:1059–71.

Li MS, Li PF, He SP, Du GG, Li G. The growth promoting mechanism of AFP on the growth of human hepatoma Bel-7402 cell line. World J Gastroenterol 2002;8:469–75.

Linden JV, Paul B, Dressler KP. A report or 104 transfusion errors in New York State. Transfusion 1993;33:21–273.

Lu KP. Pinning down cell signaling, cancer, and Alzheimer's disease. Trends Biochem Sci 2004;29:200–9.

Lu KP, Liou YC, Zhou XZ. Pinning down proline-directed phosphorylation signaling. Trends Cell Biol 2000;12:164–72.

Lubetzki-Korn I, Hirayama M, Silberberg DH, Schreiber AD, Brenner T, Abramsky O. Human AFP-rich fraction inhibits galactocerebroside antibody-mediated lysis of oligodendrocytes in vitro. Ann Neurol 1984;15:171–80.

Luft AJ, Lorscheider FL. Structural analysis of human and bovine AFP by electron microscopy, image processing, and circular dichroism. Biochemistry 1983;22:5978–81.

MacColl R, Eisele LE, Stack RF, Hauer C, Vakharia DD, Bennett A, et al. Interrelationships among secondary structure, and metal ion binding for a chemically synthesized 34-amino acid peptide derived from alpha-fetoprotein. Biochem Biophys Acta 2001; 1528:127–34.

Matsuzaki K, Harada M, Handa T, Funakoshi S, Fujü N, Yajima H, et al. Magainin 1-induced leakage of a entrapped calcein out of negatively-charged lipid vesicles. Biochem Biophys Acta 1989;981: 130–4.

Melcangi RC, Martini L, Galbiati M. Growth factors and hormones: complex interplay in the hypothalamic control of reproductive functions. Prog Neurobiol 2002;421–9.

Mickey B, Howard J. Rigidity of microtubules is increased by stabilizing agents. J Cell Biol 1995;130:909–17.

Migliaccio A, Castoria M, DiDomenico A, de Falco A. Sex steroid hormones act as growth factors. J Steroid Biochem Mol Biol 2003; 83:31–5.

Mizejewski GJ, Dias JA, Hauer CR, Henrikson KP, Gierthy J. Alpha-fetoprotein derived synthetic peptides: assay of an estrogen-modifying regulatory segment. Mol Cell Endocrinol 1996;118: 15–23.

Mizejewski GJ, MacColl R. Alpha-fetoprotein growth inhibitory peptides: potential leads for cancer therapeutics. Mol Cancer Ther 2003;2:1243–55.

Mizejewski GJ, Vonnegut M, Jacobson HI. Estradiol-activated alpha-fetoprotein suppresses the uterotropic response to estrogens. Proc Soc Natl Acad Sci U S A 1983;80:2733–7.

Mizejewski GJ, Vonnegut M, Jacobson HI. Studies of the intrinsic antiuterotropic activity of murine alpha-fetoprotein. Tumor Biol 1986;7:19–28.

Mizejewski GJ. Alpha fetoprotein structure and function: relevance to isoform, epitopes, and conformation variants. Expt Biol and Med 2001a;226:377–408.

Mizejewski GJ. Alpha-fetoprotein as a biologic response modifier: relevance to domain and subdomain structure. Proc Soc Exp Biol Med 1997a;215:333–62.

Mizejewski GJ. Growth Inhibitory Peptides. United States Patent #5,674,842. U.S. Patent Office Filing #US00567–4842A; Oct. 7, 1997b.

Mizejewski GJ. Levels of AFP during pregnancy and early infancy in normal and disease states. Obstet Gynecol Rev 2003; 58:804–26.

Mizejewski GJ. Methods of using growth inhibitory peptides. United State Patent #5, 707–963. U.S. Patent Office Filing #US005707-963A; Jan 13, 1998.

Mizejewski GJ. Review of peptides as receptor ligand drugs and their relationship to G-coupled signal transduction. Exp Opin Invest Drugs 2001b;10:1063–73.

Morinaga T, Sakai M, Wegmann TG, Tomoaki T. Primary structures of human AFP and its mRNA. Proc Natl Acad Sci U S A 1983;80: 4604–8.

Oakley BR. An abundance of tubulins. Trends Cell Biol 2000;10: 537–40.

Ohashi R, Sugimura M, Kanayama N. Estrogen administration enhances thrombin generation in rats. Thrombosis Res 2003;112: 325–8.

Onate SA, Tsai SY, Tsai M-J, O'Malley BW. Sequence and characterization of a coactivator for the steroiod hormone receptor superfamily. Science 1995;270:1354–7.

Palek J. Membrane protein and organization in normal and hemoglobinopathic red cells. Texas Report Biol Med Sect VIII Red Cell Membrane 1981;40:397–416.

Parton RG. Caveolae-from ultrastructure to molecular mechanism. Nat Rev Mol Cell Biol 2003;4:162–5.

Pelkmans L, Kartenbeck J, Helenius A. Caveolar endocytosis of simian virus 40 reveals a new two-step vesicular-transport pathway to the ER. Nat Cell Biol 2001;3:473–8.

Puca GA, Sica V. Identification of specific high affinity sites for the estradiol receptor in the erythrocyte cytoskeleton. Biochem Biophys Res Commun 1981;103:682–5.

Pyrpasopoulou A, Meier J, Maison C, Simos SD, Georgatos SD. The lamin B receptor (LBR) provides essential chromatin docking sites at the nuclear envelope. EMBO J 1996;15:7108–19.

Razandi M, Alton G, Pedram A, Ghonshani S, Webb P, Levin ER. Identification of a structural determinant necessary for the localization and function of estrogen receptor alpha at the plasma membrane. Mol Cell Biol 2003a;23:1633–46.

Razandi M, Pedram A, Park ST, Levin ER. Proximal events in signaling by plasma membrane estrogen receptors. J Biol Chem 2003b;278:2701–12.

Rebhun LI, Rosenbaum J, Lefebvre P, Smith G. Reversible restoration of the birefringence of cold-treated, isolated mitotic apparatus of surf clam eggs with chick brain tubulin. Nature (London) 1974;249: 113–5.

Rice-Evans C, Chapman D. Red blood cell biomembrane structure and deformability. Scand J Clin Lab Invest (Session III: Biochemical Approach 1981;41(Suppl. 156):99–110.

Sato K, Matsuki N, Ohno Y, Nakazawa K. Estrogens inhibit L-glutamate uptake activity of astrocytes via membrane estrogen receptor alpha. J Neurochem 2003;86:1498–505.

Savkur RS, Burris TP. The coactivator LXXLL nuclear receptor recognition motif. J Pept Res 2004;63:207–12.

Scherrer LC, Pratt WB. Association of the transformed glucocorticoid receptor with a cytoskeletal protein complex. J Steroid Biochem Mol Biol 1992;41:719–21.

Segars JH, Driggers PH. Estrogen action and cytoplasmic signaling cascades. Part I: membrane-associated signaling complexes [Review] [63 refs] Trends Endocrinol Metab 2002;13:349–54.

Shain W, Bausback D, Fiero A, Madelian V, Turner JN. Regulation of receptor-mediated shape change in astroglial cells. Glia 1992;5: 233–8.

Smith PM, Heinrich CA, Pappas S, Peluso JJ, Cowan A, White BA. Reciprocal regulation by estradiol 17-β of ezrin and cadherin–catenin complexes in pituitary GH3 cells. Endocrine 2002;17: 219–28.

Song RX, Barnes CJ, Zhang Z, Bao Y, Kumar R, Santen RJ. The role of Shc and insulin-like growth factor 1 receptor in mediating the translocation of estrogen receptor α to the plasma membrane. Proc Natl Acad Sci 2004;101:2076–81.

Sterling KM, Shah S, Kim RJ, Johnston NI, Salikhova AY, Abraham EH. Cystic fibrosis transmembrane conductance regulator in human and mouse red blood cell membranes. J Cell Biochem 2004;91:1174–82.

Stevens B, Porta S, Haak LL, Gallo V, Fields RD. Adenosine: a neuron-glial transmitter promoting myelination in the CNS in response to action potentials. Neuron 2002;36:855–68.

Sul JY, Drosz G, Givens RS, Haydon PG. Astrocytic connecting in the hippocampus. Neuron Glia Biol 2004;1:3–11.

Thatte HS, Bridges KR, Golan DE. Microtubule inhibitors differentially affect translational movement, cell surface express, and endocytosis of transferring receptors in K562 cells. J Cell Physiol 1994;160:345–57.

Torchia J, Rose DW, Inastroza J, Kamel Y, Westin S, Glass CK, et al. The transcriptional co-activator p/CIP binds CBP and mediates nuclear-receptor function. Nature 1997;387:677–84.

Treacy M, Stroup MA. Scientific forum on blood grouping serum anti-A (murine monoclonal blend) BioClone. Raritan: Ortho Diagnostic Systems; 1987. p. 1–20.

Turi A, Kill AL, Mullner N. Estrogen downregulates the number of caveolae and the level of caveolin in uterine smooth muscle. Cell Biol Int 2001;25:785–94.

Uversky NV, Kirkitadze MD, Narizhneva NV, Potekhin SA, Tomashevski AY. Structural properties of AFP from human cord serum: the protein molecule at low pH possesses all the properties of the molten globule. FEBS Lett 1995;364:165–76.

Uversky VN, Narizhneva NV, Ivanova TV, Tomashevski AY. Rigidity of human AFP tertiary structure is under ligand control. Biochemistry 1997a;36:13638–45.

Uversky VN, Narizhneva NV, Ivanova TV, Kirkitadze MD, Tomashevski AY. Ligand-free form of human AFP: evidence for the molten globule form. FEBS Lett 1997b;410:280–4.

Vakharia D, Mizejewski GJ. Human alpha-fetoprotein peptides bind estrogen receptor and estradiol and suppress breast cancer. Breast Cancer Res Treat 2000;63:41–52.

Vallette G, Vranckx R, Martin ME, Benassayag C, Nunez EA. Conformational changes in rodent and human alpha-fetoprotein: influence of fatty acids. Biochim Biophys Acta 1989; 997:302–12.

Wang Y, Chen CH. Acetylcholine receptor-enriched membrane vesicles in response to ethanol: activity and microcalorimetric studies. Biophys Chem 1992;43:51–9.

Watson CS, Campbell CH, Gametchu B. The dynamic and eleusive membrane estrogen receptor-alpha. Steroids 2002;67:429–37.

Weisenberg RC. Microtubule formation in vitro in solutions containing low calcium concentrations. Science 1972;177: 1104–5.

Williams TM, Lisanti MP. The caveolin proteins. Genome Biol 2004;5: 214–20.

Xu Y, Traystman RJ, Hurn PD, Wang MM. Membrane restraint of estrogen receptor $\alpha$ enhances estrogen-dependent nuclear localization and geneomic function. Mol Endocrinol 2004;18: 86–96.

Yamamoto F. Review: ABO blood group system – ABH oligosaccharide antigens, anti-A and anti-B, A and Bl glycosyltransferases, and ABO genes. Immunohematology 2004;20:3–12.

Yildiz A, Tomishige M, Vale RD, Selvin PR. Kinesin walks hand-over-hand. Science 2004;303:676–9.

Zafar A, Thampan RV. Association of cytoskeletal proteins with estrogen receptor in rat uterine cytosol: possible role in receptor movement into the nucleus. Biochem Mol Biol Int 1995;36: 1197–206.

Zail S. Clinical disorders of the red cll membrane skeleton. CRC Crit Rev Oncol/Hematol 1986;5:397–453.

Zhang X, Kiechle FL. Glysosphingolipids in health and disease. Ann Clin Lab Sci 2004;34:1.

Zhang ZY, Fasco MJ, Huang Z, Guengerich FP, Kaminsky LS. Human cytochromes P4501A1 and P4501A2: R-warfarin metabolism as peak. Drug Metab Dispos 1995;23:1339–46.